Disc Turbulence and Viscosity

By AXEL BRANDENBURG

Department of Mathematics, University of Newcastle upon Tyne NE1 7RU, UK

Three-dimensional simulations of hydromagnetic flows in accretion discs provide strong evidence that the turbulence in discs is driven by a magnetic instability. Some basic results of those simulations are reviewed, current shortcomings discussed, and open questions and important issues are highlighted. The main motivation behind those simulations was simply to show that turbulence is self-sustained. However, an important quantitative outcome has been the determination of the magnitude of the Shakura-Sunyaev viscosity parameter $\alpha_{\rm SS}$. It is emphasized that $\alpha_{\rm SS}$ cannot be considered a constant, as it does in fact depend on a number of factors: the magnetic field strength, the height above the midplane, and the magnitude of the velocity shear – to mention just a few. Given the availability of detailed simulations, it is now possible to address specific questions, for example what are the rates of Joule and viscous heating, where is the energy deposited, what are the values of turbulent Prandtl numbers, and how efficiently does the flow disperse and mix particles? Finally, the disc simulations have significantly affected and enhanced research in dynamo theory in different fields of astrophysics, because some of the ideas (dynamo-generated turbulence) may also apply to stars and galaxies.

---

1. Introduction

Accretion discs are a bit like waterfalls. Potential energy gets converted into kinetic and finally into thermal energy. The waterfall with the largest mass flux in Europe is Dettifoss in the northeast corner of Iceland with $\dot{M} = 1.5 \times 10^5\,{\rm kg/s}$. If Dettifoss were to be converted into a power plant, and if its efficiency was close to one hundred per cent, it would produce the equivalent of a luminosity of $L = 100\,{\rm MW}$. This is comparable with the power generated by an ordinary power plant, but less than the power produced by a nuclear power plant, which produces typically around 1000 MW. One is tempted to work out the change in water temperature per unit time due to viscous heating as the accretion stream splashes to the bottom. Equating the change of internal energy, $c_v \delta T$, with the potential energy difference suggests a temperature increase δT of only 0.1 Kelvin. This is of course consistent with common experience in that Icelandic rivers are known to be rather cold!

The mechanism by which potential energy is transferred via kinetic energy into heat is friction. However, in view of common day experience this must sound surprising, because we all know that a cup of tea would not get any warmer by stirring it. (On the contrary, but that is another matter.) Therefore, the way accretion discs produce emission is at first glance difficult to understand. However, at a second glance this is maybe not strange, because of the deep gravitational potential near the compact objects. (That does not apply to protostellar discs, but then those discs are not particularly hot either.) For Schwarzschild black holes almost 10% of the energy $E = mc^2$ of infalling material with mass m (c is the speed of light) can be extracted. On earth this is quite impossible, which is the reason why nuclear energy is here much more effective. Even on white dwarfs nuclear burning is still more effective than gravitational energy release.

There is however another much more important issue that is (or at least *was*) much more puzzling, namely the source of viscous dissipation and turbulence in discs. A related problem is the origin of enhanced (or turbulent) viscosity. With common day experience this does not appear to be a problem, because we are all used to the fact that turbulence is ubiquitous. However, this is not at all obvious in accretion discs. Convection, a strong driver of turbulence in stars, cannot be the ultimate driver of turbulence in discs, although convection may well be present in discs (e.g., Lin & Papaloizou 1980). For convection to develop, the inner layers close to the midplane have to be much hotter than the outer layers away from the midplane. However, viscous heating is the only mechanism that can possibly heat those layers. Convection transports heat away from those layers and thus cannot be responsible for setting up and maintaining a convectively unstable vertical entropy gradient. The other favourite source of turbulence is some nonlinear hydrodynamic shear instability (Dubrulle & Zahn 1991, Dubrulle 1993). However, attempts to identify such an instability in accretion discs have failed so far, and Balbus, Hawley, & Stone (1996) have shown, using simulations and analytical arguments, that purely hydrodynamic mechanisms cannot both draw energy from the shear and still transport angular momentum outwards. Although there are nonlinear shear instabilities in plane shear flow without rotation, rotation stabilizes such flows very efficiently. The simulations of Balbus, Hawley, & Stone (1996) have also shown that the onset of the nonlinear (finite amplitude) instability in the Rayleigh marginally stable case, $\partial(\varpi^2\Omega)/\partial\varpi = 0$, where ϖ is radius, can readily be simulated numerically even with relatively coarse resolution using numerical viscosities. This supports their conclusion that in the presence of rotation nonlinear hydrodynamical instabilities do not exist. There are examples of *unstable* Couette flow, but there is no example where the rotation profile is of any relevance to the case of accretion discs, i.e. where Ω decreases with radius like $\Omega \propto \varpi^{-q}$ and $0 < q < 2$.

With the rediscovery of the magnetic shearing (or magnetorotational) instability (Velikhov 1959, Chandrasekhar 1960, 1961) by Balbus & Hawley (1991, 1992) the situation has changed considerably. It is not just the fact that Balbus & Hawley have drawn attention to the importance of this instability for accretion discs, but more importantly the fact that they have shown persuasively that this, and nothing else, does actually work! In fact, Safronov (1972) did already draw attention to this instability. However, he was interested in protostellar discs and came to the conclusion that this instability would *not* work because of the low conductivity there. If his work had been in the context of accretion discs in general, maybe he would have come to another conclusion. Of course, a problem was that in the early seventies there were still many other possible sources of turbulence under consideration. One was hopeful that, if one mechanism turned out not work, some other would.

Anyway, one can say that the Balbus-Hawley instability, as it is now often called, is currently the only viable mechanism explaining turbulence in discs. Recent reviews of various aspects of the topic include those of Schramkowski & Torkelsson (1996), Brandenburg & Campbell (1997) and Balbus & Hawley (1998). The problem of cool, partially ionized protostellar discs has to be considered separately (§ 6.3). The Parker and other magnetic buoyancy instabilities must also play some role, once the Balbus-Hawley instability has developed, depending on the degree of stratification. What really matters for causing an instability similar to the Balbus-Hawley instability is simply the fact that magnetic fields couple different points in space, that would otherwise be independent. The coupling is elastic with an effective specific spring constant (per unit mass), $K = \omega_A^2 = k^2 v_A^2$, where v_A is the Alfvén speed, k some relevant wave number, and so ω_A is the Alfvén frequency. Now, if ω_A is smaller than some factor of order unity times the keplerian angular velocity Ω there is an instability. The instability appears to be much more general than that. In fact, there are now several examples where a harmonic oscillator in a keplerian orbit goes unstable if its frequency becomes comparable to or shorter than the angular frequency of the orbit. This similarity is developed further in a recent review by Brandenburg & Campbell (1997). Tidal disruption is a striking

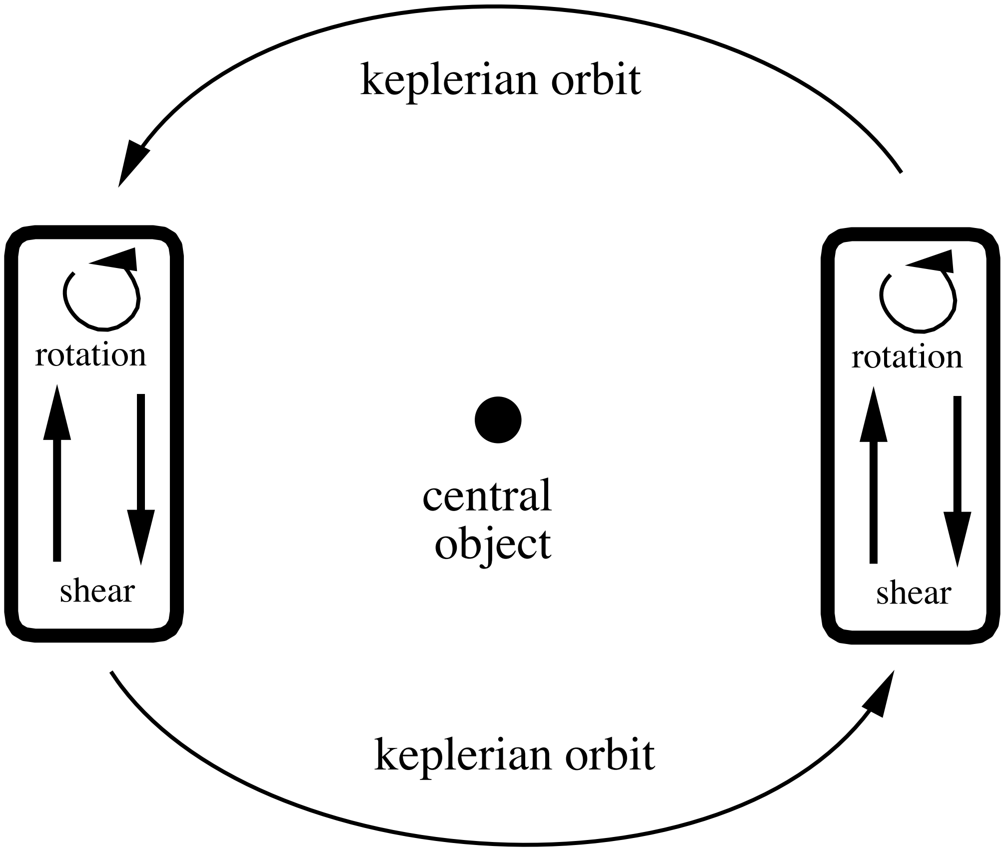

FIGURE 1. Sketch illustrating the symmetry between inward and outward directions. For the box on the right (a) the central object is to the left, so the inner parts move faster than the outer parts. For the box on the left (b) the central object is to the right. Again, the inner parts rotate faster. However, the shear flow in the two boxes (a) and (b) is exactly in the same direction. Curvature is needed to be able to tell in which direction the central object lies.

example. Here the harmonic oscillator corresponds to the radial p-mode oscillations of a star, which are of the order of 5 minutes for solar-type stars. Now if the orbital period becomes shorter or comparable to the 5 minutes oscillations the star disrupts. This can occur near black holes and is referred to as tidal disruption. This example seems to work also with g-modes. This theory has been applied to the generation of turbulence in clusters of galaxies (Balbus & Soker 1990); see also Lufkin, Balbus, & Hawley (1995) for nonlinear simulations.

The Balbus-Hawley instability is local in nature, i.e. it exists even in a local approximation. It also exists in global geometries (see Curry, Pudritz, & Sutherland 1994, Kumar, Coleman, & Kley 1994, Coleman, Kley, & Kumar 1995, Terquem & Papaloizou 1996, Ogilvie & Pringle 1996, Kitchatinov & Rüdiger 1997), but with some differences which do not affect the general conclusion. Ideally one would like to see turbulence simulations in global geometry, because the symmetry between inward and outward directions (see Fig. 1) is broken only then, and the system would 'know' whether the central object is to the left or to the right. There is work in progress by Drecker, Hollerbach, & Rüdiger (1998) trying to simulate dynamo-generated turbulence in a sphere. However, those simulations are incompressible and so the effect of gravity is only implicitly incorporated through curvature. Global turbulence simulations relevant to accretion discs have now begun to emerge. Matsumoto (private communication) has carried out global three-dimensional calculations in cylindrical geometry. However, the most detailed investigations to date have all been done using local simulations (Hawley, Gammie, & Balbus 1995, 1996, hereafter referred to as HGB95 and HGB96, Matsumoto & Tajima 1995, Brandenburg *et al.* 1995a, 1996a, hereafter BNST95 and BNST96, Stone *et al.* 1996, hereafter SHGB96). In one case (BNST96) an attempt has been made to break the symmetry between inward and outward directions by restoring terms of the order of H/R, where H is the vertical scale height and R the distance of the box from the central object.

We now discuss local calculations of accretion disc turbulence in more detail. Those simulations have in common the use of the shearing sheet approximation which, for the cross-stream (radial) direction, gives boundary conditions that are periodic with respect to fluid particles that follow the shearing motion in time. In the streamwise direction ordinary periodic boundary conditions are employed. As far as integral properties are concerned, for example the vertical magnetic flux or the total mass in the box, those quantities are conserved (assuming no mass loss in the vertical direction). This is an unfortunate restriction of all those models. The models by the various groups differ however in their vertical structure. HGB95 consider the uniform case with periodic boundary conditions in the vertical direction. SHGB96 have included vertical stratification, but they still use periodic boundary conditions in the vertical direction, although that is not a natural choice in that case. BNST95 also considered vertical stratification, but they used stress-free boundary conditions for the flow and assumed that the magnetic field is vertical on the upper and lower boundaries. The latter allows the horizontal (streamwise and cross-stream) magnetic flux to vary. This is an important property, because it enables the development of a net toroidal magnetic flux over the scale of the box. The self-consistent generation of magnetic fields, as opposed to the case of an imposed magnetic field, has been considered by BNST95, BNST96, HGB96, and SHGB96. A flow chart summarizing the relevant physical events is sketched in Fig. 2.

An important outcome of all simulations is the magnitude of the horizontal components of the Reynolds and Maxwell stresses. They are the terms that lead to angular momentum transport in the radial direction, as can be seen by inspecting the equation for angular momentum conservation in cylindrical polar coordinates, (ϖ, ϕ, z),

$$\frac{\partial}{\partial t}(\rho\varpi^2\Omega) + \boldsymbol{\nabla}\cdot[\varpi\,(\rho\boldsymbol{u}u_\phi - \boldsymbol{B}B_\phi/4\pi - \nu\rho\varpi\boldsymbol{\nabla}\Omega)] = 0. \tag{1.1}$$

When this equation is averaged we have

$$\frac{\partial}{\partial t}\langle\rho\varpi^2\Omega\rangle + \boldsymbol{\nabla}\cdot[\varpi\langle\rho\boldsymbol{u}u_\phi - \boldsymbol{B}B_\phi/4\pi - \nu\rho\varpi\boldsymbol{\nabla}\Omega\rangle] = 0. \tag{1.2}$$

In this equation the last term is small, because the microscopic viscosity ν is small. Much larger in comparison is the *turbulent* viscosity ν_t, which comes into play by *assuming* that averaged Reynolds and Maxwell stresses take a form similar to the viscous stress, but then obviously with ν being replaced by ν_t, i.e.

$$\frac{\partial}{\partial t}\langle\rho\varpi^2\Omega\rangle + \boldsymbol{\nabla}\cdot[\varpi\,(\langle\rho\boldsymbol{u}\rangle\langle u_\phi\rangle - \langle\boldsymbol{B}\rangle\langle B_\phi\rangle/4\pi - \nu_t\langle\rho\rangle\varpi\boldsymbol{\nabla}\Omega)] = 0, \tag{1.3}$$

where

$$-\nu_t\langle\rho\rangle\varpi\boldsymbol{\nabla}\Omega = \langle(\rho\boldsymbol{u})'u_\phi' - \boldsymbol{B}'B_\phi'/4\pi\rangle \equiv (\tau_{\phi\varpi}, \tau_{\phi\phi}, \tau_{\phi z}). \tag{1.4}$$

Here we have divided the various fields into mean and fluctuating parts denoted by a prime, so, for example, $\boldsymbol{u} = \langle\boldsymbol{u}\rangle + \boldsymbol{u}'$. We have also made use of the Reynolds rules (e.g.

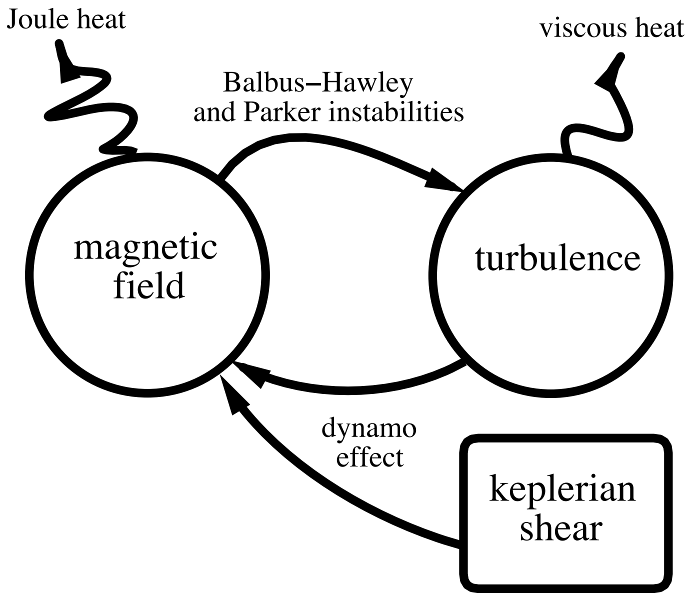

FIGURE 2. A flow chart of the different physical processes involved in accretion disc turbulence where no external magnetic field is imposed. Turbulence is generated from the magnetic field via Balbus-Hawley and Parker instabilities. The kinetic energy in the turbulence and the shear leads to the generation of magnetic fields via dynamo action. Both magnetic and kinetic energies are dissipated and produce Joule and viscous heating.

Krause & Rädler 1980) in order to write

$$\langle \rho \boldsymbol{u} u_\phi - \boldsymbol{B} B_\phi / 4\pi \rangle = \langle \rho \boldsymbol{u} \rangle \langle u_\phi \rangle - \langle \boldsymbol{B} \rangle \langle B_\phi \rangle / 4\pi + \langle (\rho \boldsymbol{u})' u'_\phi - \boldsymbol{B}' B'_\phi / 4\pi \rangle. \tag{1.5}$$

In many applications it is assumed furthermore that $\nu_t = \frac{1}{3} u_t \ell$, where u_t is the turbulent rms velocity and ℓ some suitable correlation length. Neither of these two quantities are known, but if they are assumed to be some fraction of the sound speed and the vertical scale height, i.e. that

$$\nu_t = \alpha_{\rm SS} c_s H, \tag{1.6}$$

then the famous Shakura & Sunyaev (1973) prescription is obtained; hence the subscript SS on the nondimensional coefficient $\alpha_{\rm SS}$. Using keplerian rotation, i.e. $\partial\Omega/\partial \ln \varpi = -(3/2)\Omega$, and vertical hydrostatic equilibrium, $\langle c_s^2 \rangle = \Omega^2 H^2 / 2$, we have

$$\alpha_{\rm SS} = \frac{\tau_{\varpi\phi}}{c_s H \langle \rho \rangle \frac{3}{2} \Omega} = \frac{\sqrt{2}}{3} \frac{\tau_{\varpi\phi}}{\langle \rho \rangle \langle c_s^2 \rangle} = 0.47 \times \frac{\tau_{\varpi\phi}}{\langle \rho \rangle \langle c_s^2 \rangle}. \tag{1.7}$$

Thus, $\alpha_{\rm SS}$ is 0.47 times the ratio of Reynolds and Maxwell stresses to the averaged gas pressure, $\langle p_{\rm gas} \rangle = \langle \rho \rangle \langle c_s^2 \rangle$.

In the next section we summarize the results for the coefficient $\alpha_{\rm SS}$ as found from the numerical simulations. We then discuss some aspects of the energetics and the large scale magnetic field generation. Finally we discuss a series of shortcomings of those models, some remaining questions and speculations, and then we have a look at neighbouring fields of research where cross-fertilization has occurred, or is bound to occur.

An important result for all applications is that $\alpha_{\rm SS}$ is not a constant. We discuss this now in more detail, repeating some aspects raised already in the review by Brandenburg *et al.* (1996b).

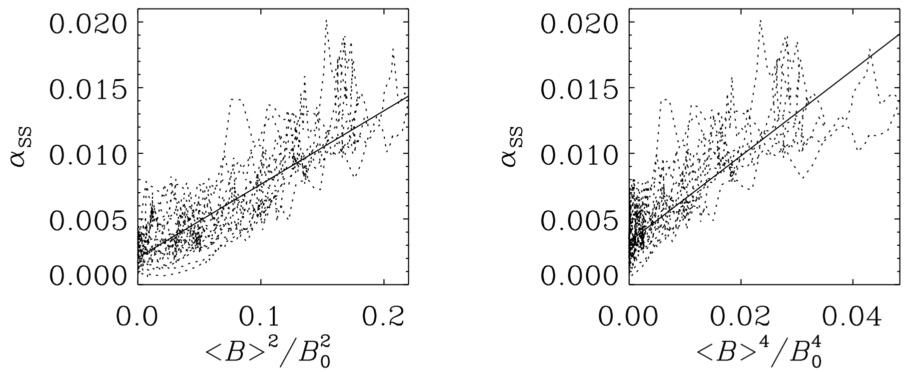

FIGURE 3. Dependence of the $\alpha_{\rm SS}$ parameter on the magnetic field strength together with a least square fit against $\langle {\rm B}\rangle^2/B_0^2$ (left hand panel) and $\langle {\rm B}\rangle^4/B_0^4$ (right hand panel).

2. Alpha is not a constant

2.1. *Alpha depends on B*

The dependence of $\alpha_{\rm SS}$ on the magnetic field strength B is probably the most important. In the models where an external magnetic field is imposed such a dependence is not surprising: the stronger the applied field, the larger the resulting stress and the larger the $\alpha_{\rm SS}$ parameter. HGB95 have found that for their runs with an imposed toroidal field the stress scales with the field like $\tau_{\varpi\phi} = 0.51\,\langle \boldsymbol{B}^2\rangle/8\pi\langle p_{\rm gas}\rangle$; see their Eq. (20). (Here and elsewhere we use a local cartesian coordinate system where x corresponds to the radial direction and y to the toroidal.) This gives

$$\alpha_{\rm SS} = 0.47\,\frac{\tau_{\varpi\phi}}{\langle p_{\rm gas}\rangle} \approx 0.12\,\frac{\langle \boldsymbol{B}^2\rangle}{B_0^2}, \tag{2.8}$$

where $B_0^2 = 4\pi\langle\rho\rangle\langle c_s^2\rangle$ is the square of the equipartition value with respect to the thermal energy.

It is remarkable that a similar dependence is found in the rather more general case where *no* external magnetic field is applied, but where an average field $\langle \boldsymbol{B}\rangle$ is generated self-consistently by dynamo action. In that case BNST96 suggested that the results for $\alpha_{\rm SS}$ can be represented in the form

$$\alpha_{\rm SS} \approx \alpha_{\rm SS}^{\rm (fit)} = \alpha_{\rm SS}^{(0)} + \alpha_{\rm SS}^{(B)}\,\frac{\langle \boldsymbol{B}\rangle^2}{B_0^2}. \tag{2.9}$$

The parameters for the fit shown in the left hand panel of figure 3 are $\alpha_{\rm SS}^{(0)} = 0.002$ and $\alpha_{\rm SS}^{(B)} = 0.06$. Note that $\alpha_{\rm SS} \neq 0$ even for vanishing mean field, $\langle \boldsymbol{B}\rangle \to 0$. In that case only the small scale magnetic field contributes to driving the turbulence (see HGB96). (The values of $\alpha_{\rm SS}^{(B)}$ given in BNST96 should be divided by a factor $\langle\rho\rangle^{-2} \approx 5.2$ due to an error in their normalization of B_0^2.) However, the data points in figure 3 appear to deviate systematically from a straight line. Indeed, a fit of the form

$$\alpha_{\rm SS} = \tilde{\alpha}_{\rm SS}^{(0)} + \tilde{\alpha}_{\rm SS}^{(B)}\,\frac{\langle \boldsymbol{B}\rangle^4}{B_0^4} \tag{2.10}$$

appears to be somewhat better in that respect. In that case we find $\tilde{\alpha}_{\rm SS}^{(0)} \approx 0.003$ and $\alpha_{\rm SS}^{(B)} \approx 0.33$. However, a dependence on $\langle \boldsymbol{B}\rangle^4$ is theoretically less plausible and the

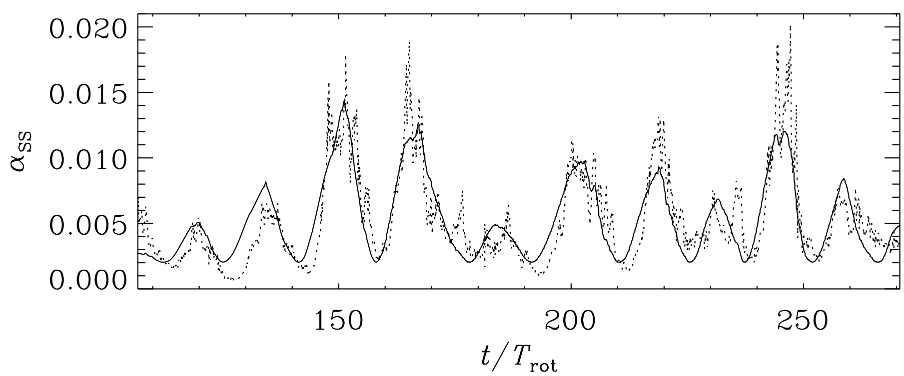

FIGURE 4. Comparison of the time dependence of $\alpha_{SS}^{(fit)}$ using the fit (2.9) (solid line) with α_{SS} (dotted line). The orbital time is $T_{rot} = 2\pi/\Omega$.

scatter in both cases is still large. The scatter is due to variations associated with the turbulence and will be discussed next.

2.2. *Alpha fluctuates in time*

The mean magnetic field depends on time and has both an average component that varies fairly gently and a fluctuating component that varies more vigorously. Therefore also α_{SS} varies with time (figure 4). Even if the mean magnetic field dependence is removed using the fit (2.9) the fluctuations of α_{SS} are still significant. The deviations from the fit, as measured by

$$\alpha_{SS}^{(fluct)}(t) = \alpha_{SS}(t) - \alpha_{SS}^{(fit)}(B(t)), \tag{2.11}$$

have no systematic time dependence, and the root-mean-square value of the fluctuations is about 0.002 for both fits, (2.9) and (2.10). Thus, we may conclude that $\alpha_{SS}(t)$ can be written in the form

$$\alpha_{SS} = \alpha_{SS}^{(fluct)} + \alpha_{SS}^{(0)} + \alpha_{SS}^{(B)} \frac{\langle \boldsymbol{B} \rangle^2}{B_0^2}, \tag{2.12}$$

where we have used eq. (2.9) for the fit. A comparison of $\alpha_{SS}(t)$ with $\alpha_{SS}^{(fluct)}(t)$ (figure 4) shows that the fit follows the evolution of the actual alpha parameter quite well, although the fit sometimes advances the evolution of α_{SS}.

2.3. *Alpha depends on z or ρ*

In the considerations above we have only looked at the vertically averaged stress. However, a disc shows significant variation in the vertical direction, so it is possible that α_{SS} also depends on z, the height above the midplane. For example, all the models of outbursts of cataclysmic variables rely on S-shaped curves for the dependence of vertically integrated disc viscosity on vertically integrated density (Meyer & Meyer-Hofmeister 1982, Cannizzo *et al.* 1988). Those models assume that α_{SS} is different on the upper and lower branches. The main reason for getting an S-shaped curve is a change in the ionization state, and thus the opacity. However, the detailed shape is model dependent. In order to calculate such a dependence from models it is assumed that α_{SS} is independent of height. Brandenburg *et al.* (1996b) pointed out that this may not be justified. In the simulations of BNST95 the variation of the magnetic field with height is relatively small compared with the variation of the density. In other words, whilst the vertical scale height of the density is about half the vertical height of the box, i.e. $H \approx 0.5L_z$, the vertical scale height of the magnetic field is certainly larger than L_z. (This may seem surprising, but it is a fairly common situation in galactic discs, where the vertical scale height of the magnetic field may well be a few kpc, much larger than the scale height of the gas which is only about 100 pc.)

The α-viscosity prescription was originally used in the context of vertically integrated models. If allowance for vertical dependence is made it is natural to continue using equations (1.4) with (1.6) and (1.7), so the vertical dependence of the horizontal component of the stress tensor, $\tau_{\varpi\phi}$, can be written in the form

$$\tau_{\varpi\phi} = -\nu_t \langle\rho\rangle_{\rm H} \varpi \frac{\partial\Omega}{\partial\varpi} \approx \tfrac{3}{2}\sqrt{2}\alpha_{\rm SS}\langle\rho\rangle_{\rm H}\langle c_s^2\rangle_{\rm H}, \tag{2.13}$$

for keplerian rotation. Here $\langle ... \rangle_{\rm H}$ denotes horizontal (xy) averages. On the other hand, $\tau_{\varpi\phi}$ does not appear to decrease significantly with height like $\langle\rho\rangle_{\rm H}$ does (see Brandenburg *et al.* 1996b). Therefore we are led to conclude that $\alpha_{\rm SS} \propto \langle\rho\rangle_{\rm H}^{-1}$ is a better approximation than just assuming $\alpha_{\rm SS}$ to be independent of z. This does in fact follow directly from eq. (2.9), if $\alpha_{\rm SS}^{(0)}$ is ignored and we assume that $\langle \boldsymbol{B}\rangle_{\rm H}$ is approximately constant with height, i.e.

$$\alpha_{\rm SS} \approx \alpha_{\rm SS}^{(\rm mag)} = \left(\alpha_{\rm SS}^{(B)} \frac{\langle \boldsymbol{B}\rangle_{\rm H}^2}{4\pi\langle c_s^2\rangle_{\rm H}}\right)\langle\rho\rangle_{\rm H}^{-1}. \tag{2.14}$$

Since the vertical scale height of $\langle \boldsymbol{B}\rangle_{\rm H}^2$ is much larger than that of $\langle\rho\rangle_{\rm H}$, and if $\langle c_s^2\rangle_{\rm H}$ is approximately constant with height, it follows that $\alpha_{\rm SS} \propto \langle\rho\rangle_{\rm H}^{-1}$. Given that $\tau_{\varpi\phi}$ is approximately independent of height, eq. (2.13) could be replaced by a perhaps more direct representation of this fact, i.e.

$$\tau_{\varpi\phi} = -\hat{\alpha}_{\rm SS}\Sigma c_s \varpi \frac{\partial\Omega}{\partial\varpi}, \tag{2.15}$$

where $\Sigma = \int_0^\infty \rho dz \approx H\langle\rho\rangle_{\rm H}(0)$, with $\langle\rho\rangle_{\rm H}(0)$ being the average density in the midplane. In our case $\hat{\alpha}_{\rm SS} \approx 0.4\alpha_{\rm SS}$. A vertical dependence of $\alpha_{\rm SS} \propto \langle\rho\rangle_{\rm H}^{-1}$, or, alternatively, the new dependence (2.15) in terms of $\hat{\alpha}_{\rm SS}$, could significantly modify various properties including the S-curves obtained using eq. (2.13).

2.4. *Alpha depends on shear and vorticity*

There is, not surprisingly, a dependence of $\alpha_{\rm SS}$ on the shear parameter $q = -\partial \ln\Omega/\partial\ln\varpi$, which measures the strength of the shear. If $q = 0$ the magnetic shearing instability shuts off, whereas in the case $q > 2$ the system is already hydrodynamically unstable (Rayleigh unstable). Abramowicz, Brandenburg, & Lasota (1996) found that $\alpha_{\rm SS}$ increases monotonically with q, keeping all other input parameters unchanged. In particular, the values of c_s and Ω itself are unchanged. Abramowicz *et al.* have pointed out that, as $q \to 2$, the turbulence became more and more vigorous until they were unable to continue the simulation. They attempted a representation using only coordinate independent quantities such as the magnitudes of the shear and vorticity tensors, σ and ω, respectively. They found that $\alpha_{\rm SS}$ is approximately proportional to the ratio of the magnitudes of the shear to viscosity tensors, i.e.

$$\langle\alpha_{\rm SS}\rangle \propto \frac{\sigma}{\omega} = \frac{q}{2-q}. \tag{2.16}$$

The ratio σ/ω vanishes for $q \to 0$ and it tends to infinity for $q \to 2$. However, calculations of Drecker, Hollerbach, & Rüdiger (1998) of the Balbus-Hawley instability in a sphere with an imposed magnetic field do not show such a singularity near $q = 2$. The origin for this discrepancy may be related to different properties of the models.

Run	comment	resolution	L_y	β^{-1}	f^{-1}	$\beta^{-1}f^{-1}$	$\tan\phi$	$\langle\alpha_{\rm SS}^{\rm (mag)}\rangle$	$\alpha_{\rm SS}^{(B)}$
O	no curv.	$31\times63\times32$	2π	0.03	2	0.06	0.07	0.004	0.07
A	no cooling	$31\times63\times32$	2π	0.01	2	0.02	0.09	0.002	0.09
B	short run	$31\times63\times32$	2π	0.01	4	0.02	0.08	0.002	0.15
C	high res.	$63\times127\times64$	2π	0.01	8	0.03	0.11	0.004	0.41
D	aspect rat.	$127\times63\times32$	4π	0.02	3	0.04	0.09	0.004	0.12
E	aspect rat.	$255\times63\times32$	8π	0.01	4	0.04	0.08	0.003	0.16

TABLE 1. Summary of parameters entering the equation for the value of $\alpha_{\rm SS}$. Note that in Run A cooling was turned off, so the temperature and hence the disc scale height increase with time. Therefore the temporal averages given for this run cannot readily be compared with those of the other runs. In all runs, except Run O, curvature terms of the form $1/R$ have been restored, so there is a nonvanishing mass accretion rate; see BNST96. However, within statistical errors, the values in the table are probably unaffected by this.

A dependence of the form (2.16) has several implications. First of all, it may provide a mechanism for limiting the disc thickness. A thick, pressure-supported disc (Abramowicz, Calvani, & Nobili 1980) is assumed to have constant angular momentum, i.e. $q\to2$, so according to eq. (2.16) the viscosity will be very large, and one expects a large accretion velocity which would then rapidly lead to a state where the centrifugal force balances gravity as described by thin disc theory. The second example where eq. (2.16) could be applied is near black holes. Assuming that the dependence on σ/ω carries over to the relativistic regime near black holes, where σ/ω increases considerably, eq. (2.16) would predict a systematic increase of $\alpha_{\rm SS}$ towards the inner parts of the disc, which tend to contribute strongest to the observed spectrum.

2.5. *Alpha depends on the numerical resolution*

Finally we mention the fact that our results for the averaged values of the mean magnetic field, $\langle\boldsymbol{B}^2\rangle$, and therefore also of $\alpha_{\rm SS}$, are not yet converged and tend to increase as the number of mesh points is increased. BNST96 found for the time averages $\langle\alpha_{\rm SS}\rangle=0.005$ for $31\times63\times32$ meshpoints and $\langle\alpha_{\rm SS}\rangle=0.007$ for $63\times126\times64$ meshpoints. The magnetic contribution to $\alpha_{\rm SS}$, see eq. (1.4), can be written as

$$\langle\alpha_{\rm SS}^{\rm (mag)}\rangle\equiv-0.47\times\frac{\langle B'_\varpi B'_\phi\rangle}{4\pi\langle\rho\rangle\langle c_s^2\rangle}=-0.47\times\frac{\langle B'_\varpi B'_\phi\rangle}{\langle\boldsymbol{B}^2\rangle}\,\frac{\langle\boldsymbol{B}^2\rangle}{\langle\boldsymbol{B}\rangle^2}\,\frac{\langle\boldsymbol{B}\rangle^2}{4\pi\langle\rho\rangle\langle c_s^2\rangle};\tag{2.17}$$

see (1.7). We now introduce the plasma-beta, $\beta=2B_0^2/\langle\boldsymbol{B}\rangle^2$, the tangent of the pitch angle, $\tan\phi\equiv-\langle B'_\varpi B'_\phi\rangle/\langle\boldsymbol{B}^2\rangle\approx-B'_\varpi/B'_\phi$, and the filling factor $f=\langle\boldsymbol{B}\rangle^2/\langle\boldsymbol{B}^2\rangle$. With those definitions we can express $\langle\alpha_{\rm SS}^{\rm (mag)}\rangle$ in the form

$$\langle\alpha_{\rm SS}^{\rm (mag)}\rangle=0.94\,\beta^{-1}f^{-1}\tan\phi.\tag{2.18}$$

Except for the offset $\alpha_{\rm SS}^{(0)}$ in eq. (2.9), eq. (2.17) is similar to eq. (2.9) if we identify $\alpha_{\rm SS}^{\rm (B)}$ with $f^{-1}\tan\phi$, i.e.

$$\alpha_{\rm SS}^{(B)}=0.47\,f^{-1}\tan\phi.\tag{2.19}$$

This means that if eq. (2.9) is valid, the product of pitch and the inverse filling factor should be constant. Alternatively, if eq. (2.10) is valid, the product of pitch and inverse filling factor should increase with increasing field strength proportionally to β^{-1}. Table 2.5 summarizes some of the relevant parameters of the simulations of BNST96. However, the results do not confirm either of the two possibilities mentioned above. Instead, $\alpha_{\rm SS}^{(B)}$ is roughly proportional f^{-1} and only weakly dependent on $\tan\phi$.

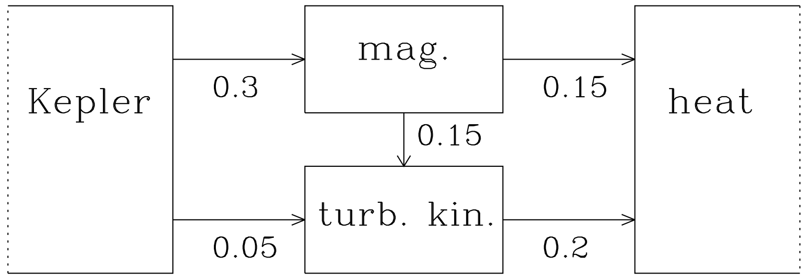

FIGURE 5. Diagram showing the energy fluxes between the various energy reservoirs. Most of the energy is being tapped from the keplerian shear via Maxwell stresses. However, the magnetic field drives turbulent motions which contribute significantly to heating the disc. The numbers denote energy fluxes in units of the average magnetic energy times Ω, as estimated from the simulation data. (Adapted from BNST95.)

3. Energetics and energy fluxes

Since we are dealing here with a magnetic instability it is not surprising that most of the energy that is tapped from the keplerian shear motion goes into magnetic energy. Subsequently, however, there is a conversion of magnetic energy into turbulent kinetic energy. This sink of magnetic energy lowers the amount of energy that has to go into Joule heating. The simulations of BNST95 have allowed us to estimate the relative magnitudes of the various energy fluxes. They found that, although most of the energy does indeed go first into magnetic energy, the energies that are eventually dissipated by Joule and viscous heating are more or less equal. The relative importance of the two heating processes may have consequences for the deposition of thermal energy into electrons and ions, which will be discussed next.

3.1. *Deposition of energy via Joule and viscous heating*

The relative importance of Joule and viscous heating is of particular significance for discs in active galactic nuclei, because there electrons are thought to be of lower temperature than the ions. On the other hand, if the Balbus-Hawley instability is really responsible for driving the turbulence one might expect that most of the heating takes place via Joule heating, which would deposit energy predominantly into the electron component.

However, there is typically a flux of energy from the magnetic field into the turbulent kinetic energy. This extra gain of kinetic energy due to the Balbus-Hawley and possibly other (secondary) instabilities enhances the viscous flux of energy and lowers the flux due to Joule heating; see figure 5. An important question is then whether the ratio between viscous and Joule heating depends on the microscopic magnetic Prandtl number $\mathrm{Pr}_M = \nu/\eta$, where ν is the kinematic viscosity and η the magnetic diffusivity. Note that these are not turbulent, but microscopic (i.e. 'molecular' or rather 'atomic') values for the viscosity and magnetic diffusivity. The expressions for viscous and Joule heating per unit volume are

$$Q_{\mathrm{visc}} = 2\nu\rho\boldsymbol{S}^2, \quad Q_{\mathrm{Joule}} = \eta\mu_0\boldsymbol{J}^2, \tag{3.20}$$

where $\boldsymbol{S}$ is the strain tensor and $\boldsymbol{J}$ the electric current. For example, if Pr_M is large, i.e. $\nu \gg \eta$, one might expect $Q_{\mathrm{visc}} \gg Q_{\mathrm{Joule}}$. However, a small value of η does not necessarily imply that $\eta\boldsymbol{J}^2$ is small, because $\boldsymbol{J}^2$ increases when η decreases. This can be seen in simulations of coronal heating via nanoflares (Galsgaard & Nordlund 1996). The same is also true for viscous heating. Thus, one expects that the ratio $Q_{\rm visc}/Q_{\rm Joule}$ is roughly independent of Pr_M. Instead, $Q_{\rm visc}/Q_{\rm Joule}$ depends primarily on the rates at which kinetic and magnetic energies are tapped from the keplerian shear, and also on the rate at which magnetic energy can be converted into turbulent kinetic energy. If $F_{\rm kin}=\frac{3}{2}\Omega\langle\rho u_\varpi u_\phi\rangle$ and $F_{\rm mag}=-\frac{3}{2}\Omega\langle B_\varpi B_\phi\rangle/\mu_0$ are the rates at which kinetic and magnetic energy is being tapped from the shear, and if $W_{\rm Lor}=\int\boldsymbol{u}\cdot(\boldsymbol{J}\times\boldsymbol{B})\,dV$ is the work done by the Lorentz force ($W_{\rm Lor}>0$ in the present case, where the turbulence is driven by the field), then we have on average in the statistically steady state

$$\tilde{Q}_{\rm visc}=F_{\rm kin}+W_{\rm Lor}, \tag{3.21}$$

$$Q_{\rm Joule}=F_{\rm mag}-W_{\rm Lor}. \tag{3.22}$$

where $\tilde{Q}_{\rm visc}=Q_{\rm visc}+Q_{\rm comp}$ is the heating from viscous dissipation and compressional heating, $Q_{\rm comp}=-\langle p\boldsymbol{\nabla}\cdot\boldsymbol{u}\rangle$; see BNST95. We should add here that due to discretization errors and finite time averages the actual numbers do not quite match this relation. This is also because certain integral relations that enter in the derivation of the relations above are numerically only approximately satisfied. Therefore the heating rates given in figure 5 have been adjusted in order to avoid confusion or misinterpretation.

It remains unclear how large $W_{\rm Lor}$ can be. If $W_{\rm Lor}/F_{\rm mag}$ approaches unity we have $Q_{\rm Joule}\ll Q_{\rm visc}$ and so most of the energy is dissipated in the 'conventional' way via viscous heating, which means that at first instance the ions will be heated. On the other hand, if $W_{\rm Lor}/F_{\rm mag}$ were small, most of the energy would go via Joule heating into the electrons. This may lead to a problem in that in active galactic nuclei the electron temperatures are observed to be smaller than the ion temperatures. However, as pointed out by Shapiro, Lightman, & Eardley (1976), the electrons cool faster, so even in that case the electron temperatures could well be below the ion temperatures. A recent discussion of this in connection with advection dominated accretion flows can be found in Bisnovatyi-Kogan & Lovelace (1997). Thus, the detailed properties of energy deposition unfortunately do not seem to lead to stringent observational constraints.

3.2. *The turbulent magnetic Prandtl number*

Although the microscopic Prandtl numbers may not be very important as far as macroscopic, or averaged, properties are concerned, the *turbulent* (ordinary and magnetic) Prandtl numbers may be be useful when trying to model large scale properties of the disc.

The value of the turbulent magnetic Prandtl number, $\mathrm{Pr}_M^{\rm (turb)}=\nu_t/\eta_t$, is important for the dragging of field lines from the interstellar medium into the disc. There is the common conception that the radial accretion flow will drag field lines to the inner parts of the disc. On the other hand, it is well known that this process has to compete against magnetic diffusion outwards (van Ballegooijen 1989, see also Pringle 1993 and Lubow, Papaloizou, & Pringle 1994). Efficient field line dragging may occur only for $\mathrm{Pr}_M^{\rm (turb)}\gg 1$. For $\mathrm{Pr}_M^{\rm (turb)}=1$ the final result is not clear, the more so because the turbulent magnetic diffusion is really a tensor. More work is needed to determine the nature of field line slippage and viscous accretion flows.

3.3. *The turbulent Prandtl number*

The magnitude of the turbulent Prandtl number, $\mathrm{Pr}^{\rm (turb)}\equiv\chi_t/\nu_t$, where χ_t is the turbulent thermal diffusivity, could also play an important role. In many models of the vertical stratification of discs the effects of turbulent heat transport are neglected altogether and only the effects of radiation are taken into account.

Since the temperature in the boxes considered by BNST95 and BNST96 is almost independent of height, the specific entropy increases with height. According to mixing length theory (e.g. Rüdiger 1989) this must then lead to a turbulent enthalpy (or convective) flux, $\boldsymbol{F}_{\rm conv}$, towards the midplane, where

$$\boldsymbol{F}_{\rm conv} = -\chi_t \langle\rho\rangle\langle T\rangle \boldsymbol{\nabla}\langle s\rangle. \tag{3.23}$$

The value of χ_t can be estimated, because all other quantities in eq. (3.23) are known. The result is that $\mathrm{Pr}^{(\rm turb)} \approx 0.1$. This value is relatively small, perhaps too small to explain significant modifications of the radial temperature dependence of this (Fröhlich & Schultz 1996). This value of χ_t should be compared with the radiative value, which cannot be done in the present simulations where radiation transport is not included. Furthermore, it is not clear that the results carry over to the case where the turbulence transports heat outwards and not inwards as in the present models.

3.4. *Compressive versus vortical motions*

For the Balbus-Hawley instability compressibility is not an essential ingredient (e.g. Ogilvie, & Pringle 1996). One may therefore expect compressibility to be weak in the simulations. On the other hand, the simulations are compressible and shocks may form, especially away from the midplane where the density is low and the Mach number high. It is therefore of interest to assess the relative importance of compressive and vortical motions. On the one hand, this is just another means of characterizing the type of motion taking place in the disc. On the other hand, the relative importance of compressive and vortical motions may have important implications for certain secondary effects, such as photon damping of compressive MHD waves (Agol, & Krolik 1998).

One way of quantifying the relative importance of compressive and vortical motions is by measuring the root-mean-square values of vorticity and velocity divergence. For example, in compressible convection the rms velocity divergence is about 10% of the rms vorticity (Brandenburg *et al.* 1996c). In accretion disc turbulence this ratio can easily be much larger, as can be seen from the first panel of figure 6 where we have plotted the ratio $(\boldsymbol{\nabla}\cdot\boldsymbol{u})_{\rm rms}/\omega_{\rm rms}$ separately for each layer. Here, $(\boldsymbol{\nabla}\cdot\boldsymbol{u})_{\rm rms} = \langle(\boldsymbol{\nabla}\cdot\boldsymbol{u})^2\rangle^{1/2}$ and $\omega_{\rm rms} = \langle\boldsymbol{\omega}^2\rangle^{1/2}$ are the rms values of velocity divergence and vorticity. One sees that this ratio is largest close to the midplane, where values between 0.4 and 0.7 are reached. Thus, compressive effects are actually important near the midplane, even though the Mach number is low there.

Another way of characterizing the flow is by separating it explicitly into vortical and compressive components,

$$\boldsymbol{u} = \boldsymbol{u}_{\rm vort} + \boldsymbol{u}_{\rm comp}. \tag{3.24}$$

By expressing the two contributions in terms of vector and scalar potentials, $\boldsymbol{u}_{\rm comp} = \boldsymbol{\nabla}\times\boldsymbol{\psi}$ and $\boldsymbol{u}_{\rm vort} = \boldsymbol{\nabla}\phi$, one can see that $\boldsymbol{\nabla}\times\boldsymbol{u} = \boldsymbol{\nabla}\times\boldsymbol{u}_{\rm vort}$ and $\boldsymbol{\nabla}\cdot\boldsymbol{u} = \boldsymbol{\nabla}\cdot\boldsymbol{u}_{\rm comp}$. In the second panel of figure 6 we show velocity powerspectra separately for vortical and compressive components of $\boldsymbol{u}$. The ratio between the typical magnitudes of the spectral energies of vortical and compressive components of $\boldsymbol{u}$ is about ten, confirming that the ratio of the typical magnitudes of the velocity is around three. The spectra are too short to identify an inertial range, but even for the largest scales the slopes in the curves are typically k^{-2} or even steeper.

Finally, in figure 7 we look at the vertical profiles of rms velocity and Alfvén speed and the vortical and compressive Taylor microscales, $u_{\rm rms}/\omega_{\rm rms}$ and $u_{\rm rms}/(\boldsymbol{\nabla}\cdot\boldsymbol{u})_{\rm rms}$,

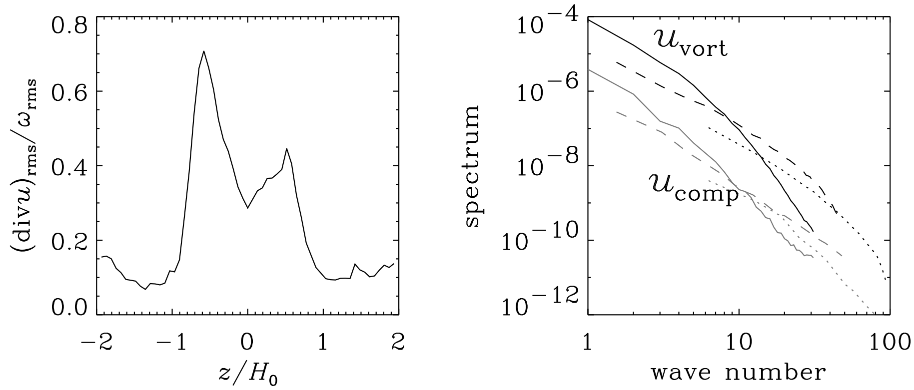

FIGURE 6. Left hand panel: ratio of rms velocity divergence to rms vorticity. Right hand panel: velocity power spectra of vortical and compressive components. Solid lines refer to power spectra taken in the y direction, whilst dotted and dashed lines refer to the x and z directions. The three spectra for the compressive motions are plotted as grey lines.

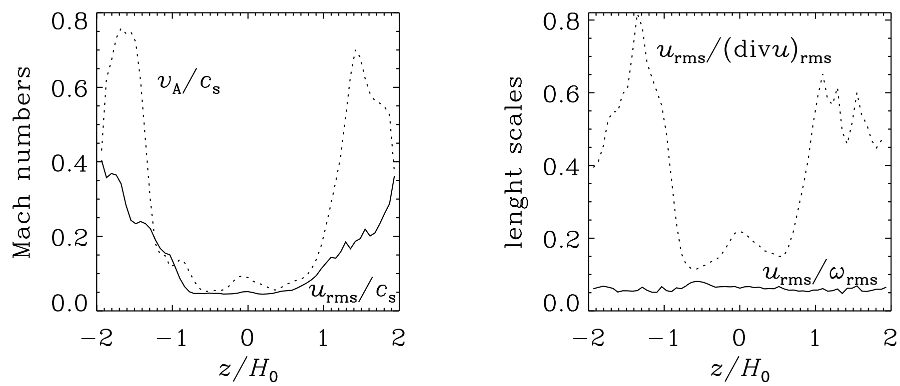

FIGURE 7. Left hand panel: the turbulent Mach number u_{rms}/c_s (solid line), and turbulent magnetic Mach number v_A/c_s (dotted line), as functions of height. Right hand panel: vortical and compressive Taylor microscales (see text).

respectively. We find that $u_{\mathrm{rms}}/\omega_{\mathrm{rms}}$ varies very little with height, whilst the scale $u_{\mathrm{rms}}/(\boldsymbol{\nabla}\cdot\boldsymbol{u})_{\mathrm{rms}}$ is largest away from the midplane and smallest near the midplane.

4. The importance of modelling the large scale field

We have seen that the Shakura-Sunyaev alpha, α_{SS}, remains time dependent and varies with the large scale magnetic field; see equations (2.9) or (2.10). This type of variation is ignored in the standard accretion disc model – even if time dependence is essential, like in models for cataclysmic variables. In order to include this effect one would need to solve a set of model equations for the dynamo. We begin by discussing first the basic conclusions gained from the simulations and then turn to their phenomenological description.

It is remarkable that in the local simulations not only a small scale magnetic field is generated, but also a large scale field. However, the generated large scale magnetic field may be sensitive to the magnetic boundaries adopted, because the scales over which the

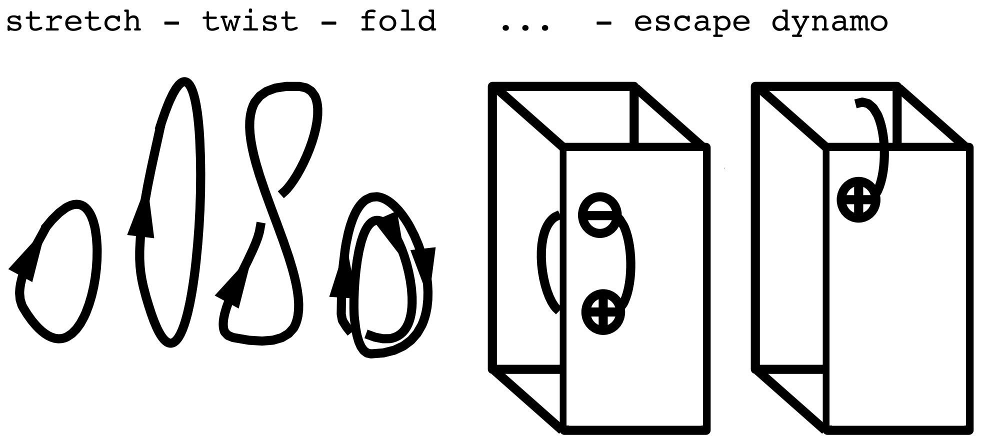

FIGURE 8. Sketch illustrating the enhancement of small scale flux from a stretch–twist–fold dynamo and the subsequent escape of flux contributing to a net horizontal field as long as the flux loop has escaped only partly through the boundary.

magnetic field varies is comparable with the size of the computational domain. In order to assess the sensitivity to changes in the magnetic boundary conditions we now compare two local simulations carried out with two rather 'orthogonal' conditions on $z=\pm L_z$,

$$B_x = B_y = \frac{\partial B_z}{\partial z} = 0 \quad \text{(vertical field condition)}, \tag{4.25}$$

$$\frac{\partial B_x}{\partial z} = \frac{\partial B_y}{\partial z} = B_z = 0 \quad \text{(perfect conductor condition)}. \tag{4.26}$$

The vertical field condition, eq. (4.25), imitates a vacuum boundary condition. However, for a proper vacuum boundary condition one would have to match the solution to a potential field solution, $\boldsymbol{B}=\boldsymbol{\nabla}\phi$ with $\nabla^2\phi=0$. This leads to a nonlocal condition in that the condition at one point depends on the field at all other points on the boundary. The condition becomes local in spectral space (e.g. Krause & Rädler 1980), and is usually implemented using Fourier transforms. However, the shearing sheet condition precludes the use of Fourier transforms in the cross-stream direction. A possible alternative would be to transform onto a nonorthogonal grid and to apply Fourier transform in the (inclined) direction in which the mesh is periodic. This approach has been adopted by Charles Gammie (private communication) in order to solve the Poisson equation in simulations with self-gravity. Thus, in view of those complications, the vertical field condition eq. (4.25) is a sensible compromise – good enough for the purpose of a local model. In this connection it should be remembered that in a local model the potential field condition has its own unrealistic feature in that the field decays exponentially with height and not algebraically. Also, the medium in the disc corona is not insulating. A better, albeit much harder, approach is to solve for a force-free field outside. Anyway, the vertical field condition used so far can be physically motivated by saying that near the boundaries magnetic buoyancy tends to make the field emerge vertically from the boundary. This vertical field condition has been used extensively in simulations of magnetoconvection (e.g. Hurlburt & Toomre 1988).

Both, the vertical field condition as well as the vacuum condition have the property that toroidal flux is no longer conserved. This is a crucial property of a large scale dynamo. In figure 8 we illustrate why this is important. Suppose the dynamo in the disc generates only closed small-scale loops. A possible mechanism for this is the stretch–twist–fold

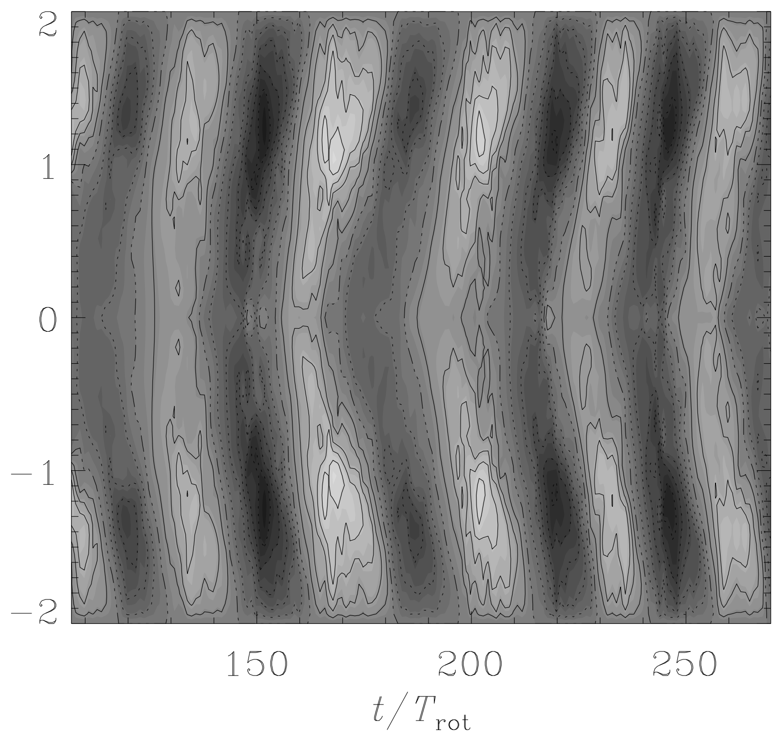

FIGURE 9. Space-time diagram of the averaged toroidal magnetic field in a simulation using the vertical magnetic field boundary condition. By imposing boundary conditions on $z = 0$ the field has been made strictly symmetric about the midplane. The field is oscillatory with a typical period of about 30 orbits.

dynamo (Vainshtein, & Zeldovich 1972), which regenerates new field loops with twice the flux after each iteration. Since the loops are closed they contribute no net flux over the scale of the box, but when such a loop escapes through the boundary there will be a nonvanishing net flux. In that sense one may call this a stretch–twist–fold–*escape* dynamo.

4.1. *The effect of boundary conditions in local simulations*

For most of the calculations carried out so far magnetic boundary conditions have been used that force the magnetic field to be vertical on the upper and lower boundaries. Technically this has the advantage that thus the horizontal components of the magnetic flux, i.e. the mean magnetic fields $\langle B_x \rangle$ and $\langle B_y \rangle$, are not restricted and can evolve freely (BNST95). In that case we find an oscillatory magnetic field, a space-time diagram of which is given in figure 9. Those results should be contrasted with the case of the perfect conductor boundary condition, of which a space-time diagram is shown in figure 10. We restarted this simulation from a previous snapshot obtained using the vertical field boundary condition. Therefore the initial condition was of even parity, and the field continued to show signs of oscillatory behaviour for the first ten orbits, but then the oscillations died away and the field began to settle into an antisymmetric configuration without cycles and yet finite amplitude.

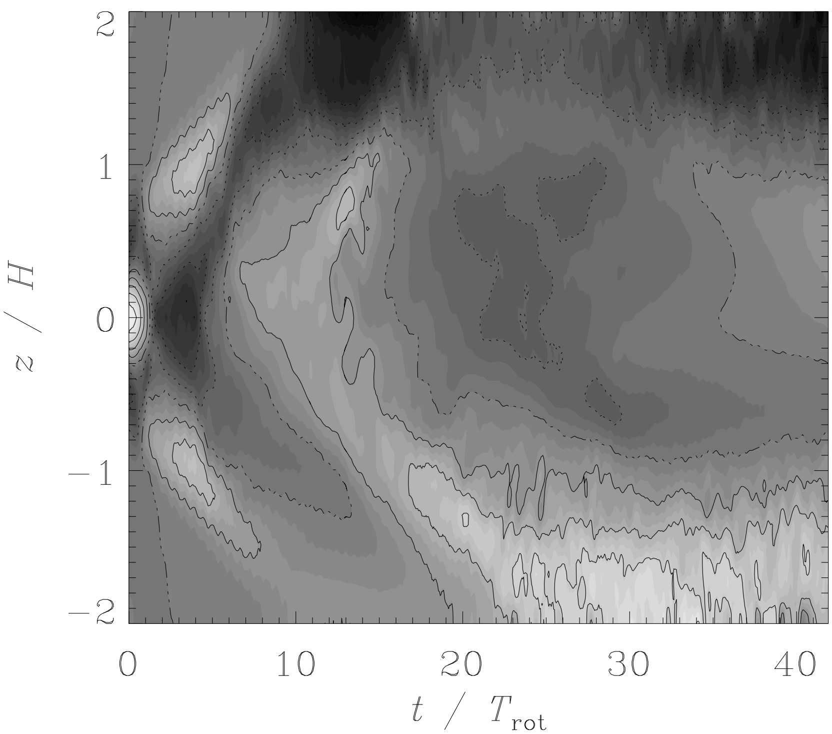

FIGURE 10. Space-time diagram of the averaged toroidal magnetic field in a simulation using the perfect conductor boundary condition for the magnetic field. The initial condition was taken from a snapshot of a simulation with the vertical field condition, where the field was oscillatory and of even parity. Until $t = 10\,T_{\rm rot}$ the field continued to show signs of oscillatory behaviour, but it then turned to be of odd parity about $z = 0$ without being oscillatory.

In both cases a large scale field is generated. There are two main differences between the two cases with perfect conductor and with vertical field boundary conditions. Firstly, for the vertical field condition the toroidal field is of approximately even parity about the midplane, $z = 0$, whereas in the perfect conductor case the field is of approximately odd parity about $z = 0$. Secondly, the field is oscillatory if a vertical field condition is used, but non-oscillatory in the other case. Thus, obviously the behaviour of the magnetic field is quite dependent on the precise boundary conditions for the magnetic field. Thus, one might deduce that no sensible conclusions can be drawn from current local simulations. However, in the following we shall point out that this behaviour is quite consistent with what is expected from mean-field dynamo models in the same geometry. This may lend some support to the interpretation of those results in terms of mean-field models. However, it remains true that issues of whether or not the field is oscillatory require global modelling. We return to the results for global models of mean-field dynamos at the end of the next section.

4.2. *The effect of boundary conditions in mean-field models*

A way to understand large scale magnetic field generation in astrophysical bodies is the concept of an $\alpha\Omega$-dynamo. Here the dynamo alpha, $\alpha_{\rm dyn}$ (with dimensions of velocity),

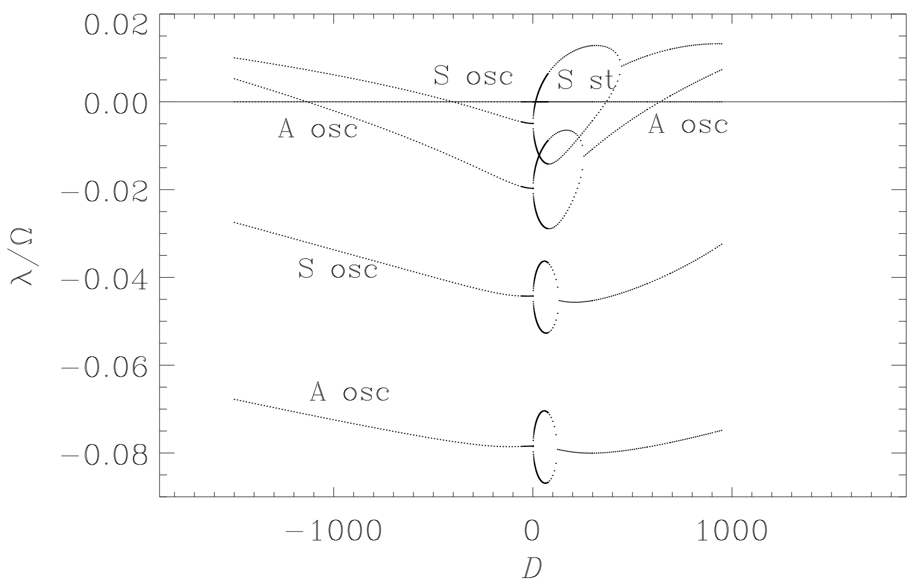

FIGURE 11. The first largest (normalized) eigenvalues, λ/Ω, of an $\alpha\Omega$ dynamo in a cartesian box with vertical magnetic field boundary conditions at top and bottom. For negative dynamo numbers, $D<0$, the first excited mode has symmetric parity and is oscillatory (S osc) near $D=-400$, which is in qualitative agreement with the simulations.

is quite distinct from the nondimensional $\alpha_{\rm SS}$ parameter. The relevant dynamo equation is obtained by averaging the induction equation. In the resulting equations there are two important parameters, the α-effect and the turbulent magnetic diffusivity, η_t. For the particular simulations of BNST96 there is now quantitative information concerning the magnitudes of those two parameters. Recent work by Brandenburg & Donner (1997) and Brandenburg & Sokoloff (1998) suggests that $\alpha_{\rm dyn}\approx\mp0.001\Omega H$ (in the upper and lower disc planes, respectively) and $\eta_t\approx(0.003-0.008)\Omega H^2$. Note that the sign of $\alpha_{\rm dyn}$ changes at the midplane. This antisymmetry is connected with the fact that $\alpha_{\rm dyn}$ is a pseudoscalar, i.e. it changes sign under a coordinate transformation with respect to reflection.

When solving the mean-field dynamo equations it is found that the lowest wave numbers of the magnetic field, corresponding to the largest possible scales, dominate the problem. Therefore boundary effects play an important role. For example, the nature of magnetic cycles is expected to depend on the geometry (local/global) and on boundary conditions. To address those issues we now compare our local simulations with mean-field dynamo models using the two boundary conditions (4.25) and (4.26).

We have calculated the first few largest eigenvalues, λ, of the mean-field dynamo equations using as boundary conditions either (4.25), see figure 11, or (4.26), see figure 12, and $\alpha_{\rm dyn}(z)=\alpha_0\,(z/H)$. The relevant equations used in the calculation can be found in Brandenburg & Campbell (1997) and Brandenburg & Donner (1997), for example.

For oscillatory solutions there is a pair of complex conjugate eigenvalues, with frequencies $\pm{\rm Im}\lambda$. As the dynamo number, $D=q\alpha_0\Omega H^3/\eta_t^2$, changes those two modes with the same growth rate ${\rm Re}\lambda$ may split into two non-oscillatory modes. They are steady when the growth rate vanishes, so we refer to those modes as ‘S st’ and ‘A st’ for sym-

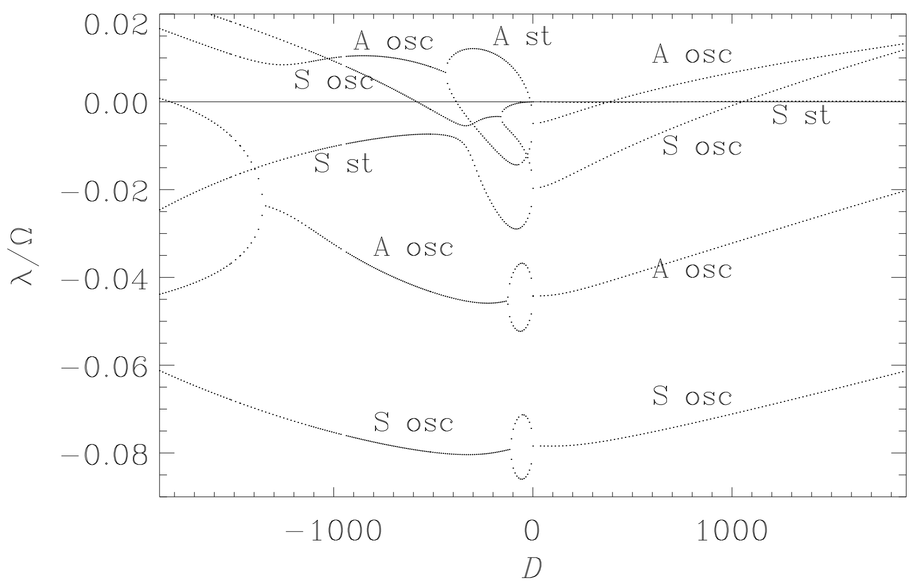

FIGURE 12. The first largest (normalized) eigenvalues, λ/Ω, of an $\alpha\Omega$ dynamo in a cartesian box with perfect conductor boundary conditions at top and bottom. For negative dynamo numbers, $D<0$, the first excited mode is now antisymmetric about $z=0$ and the field is nonoscillatory (A st) near $D=-10$, which is again in qualitative agreement with the simulations for this type of boundary condition.

metric and antisymmetric fields, respectively. For negative values of α_0, i.e. for $D<0$, we find that the first excited mode is symmetric and oscillatory (S osc) when (4.25) is used (see figure 11) and antisymmetric and non-oscillatory (A st) when (4.26) is used (see figure 12). Both of these properties agree with the results of the local turbulence simulations.

One could think of many reasons why the $\alpha\Omega$-dynamo may not provide an adequate description of the magnetic field behaviour in accretion discs. For example, there are indications that $\alpha_{\rm dyn}$ and η_t may be wavenumber dependent (Brandenburg & Sokoloff 1998) and, of course, the effects of fluctuations are ignored. Nevertheless, it does allow some explicit modelling of the magnetic field, which otherwise would have been assumed to vanish altogether, and it does reproduce some gross properties of the magnetic field found in fully three-dimensional accretion disc simulations.

5. Deficiencies of current simulations

We have already mentioned briefly some main deficiencies of present models, namely the local nature and limited extent of the simulations in the vertical, radial and toroidal directions. Let us now discuss both of these restrictions in more detail.

5.1. *The limited vertical extent of the box*

Most of the published models extend to just a few density scale heights H. Whilst cooling keeps the value of H close to the initial value, any heating of the disc tends to increase the value of H and would therefore lower the number of scale heights within the box. At the same time, as we have already discussed, the magnetic field shows no signs of levelling off towards large heights. On the contrary, once the field has reached the upper and lower boundaries it starts to feel the boundaries and there are signs of an artifactual increase of the magnetic field near the boundaries (Nordlund, private communication).

Future work has to reveal, (i) what is the true vertical magnetic field distribution in discs and, (ii) how can that be modelled using local simulations. An important computational problem here is the fact that the density drops significantly towards the upper and lower boundaries, whilst the magnetic field has hardly changed. Consequently the Alfvén speed increases significantly towards the low plasma-beta corona of the disc, making the time step very short.

Recently, Matsumoto (private communication) has performed simulations of a box that covered about ten scale heights with a density contrast of about 1 : 1000 between the upper edge of the box and the midplane. He considers the case where z/ϖ reaches values of order unity and so he has to allow for deviations from the simple gravity law $g_z = -\Omega^2 z$. In his case the main objective was to study the effects resulting from the Parker instability. However at the moment his simulations cover only the first ten orbits.

5.2. *Geometry and radial boundary conditions*

An important restriction from the assumption of (sliding) periodic boundary conditions in the radial direction is the fact that the mass in the box cannot change, except in principle for vertical mass loss, which cannot occur in the present models either. Hence, with sliding periodic boundary conditions there can be no local accumulation of matter by having more input from the outside and less output towards the inner parts of the disc. Furthermore, the averaged vertical magnetic field is strictly conserved and since it is zero initially, it remains so for all times. Both of these problems can be removed by going to a model in cylindrical geometry with open boundary conditions in the radial direction. However, some experience needs to be gained to make sure that a model with open boundary conditions is stable.

5.3. *The toroidal extent of the box*

The boxes used by HGB95 and BNST95 had usually a toroidal extent of about six vertical scale heights. For shorter boxes the turbulence does not seem to have enough freedom to develop and the resulting values of $\alpha_{\rm SS}$ are smaller than for larger boxes. Making the box much longer does not seem to have a strong effect on the value of $\alpha_{\rm SS}$; see BNST96 and figure 13, where we have reproduced images of vertical vorticity in a horizontal plane $z = H$ for runs with three different aspect ratios and, for the largest aspect ratio, two different values for the resolution in the longitudinal direction.

In the recent simulations of Matsumoto (private information) the toroidal extent has been increased to almost twenty vertical scale heights. Note that the Parker instability has wavelengths in the toroidal direction of ten or more density scale heights. It is therefore only now in the new simulations of Matsumoto that the Parker instability can fully develop. However, the toroidal extent alone was not sufficient, but it was probably the combination of increased toroidal and vertical extent together with an initially strong magnetic field (his plasma beta was initially unity). It will be important to see the full results of those simulations. The only problem is that there are at present difficulties with extending the simulations for much longer than about ten orbits. Part of this is difficulty is presumably the fact that the small size of the time step becomes very restrictive as the plasma beta becomes smaller than unity. Another difficulty is the fact that pressure gradients become ineffective in responding to fluid expansion or compression that are governed by the continuity equation. This may locally result in very low temperatures, which are difficult to handle if there are not enough mesh points.

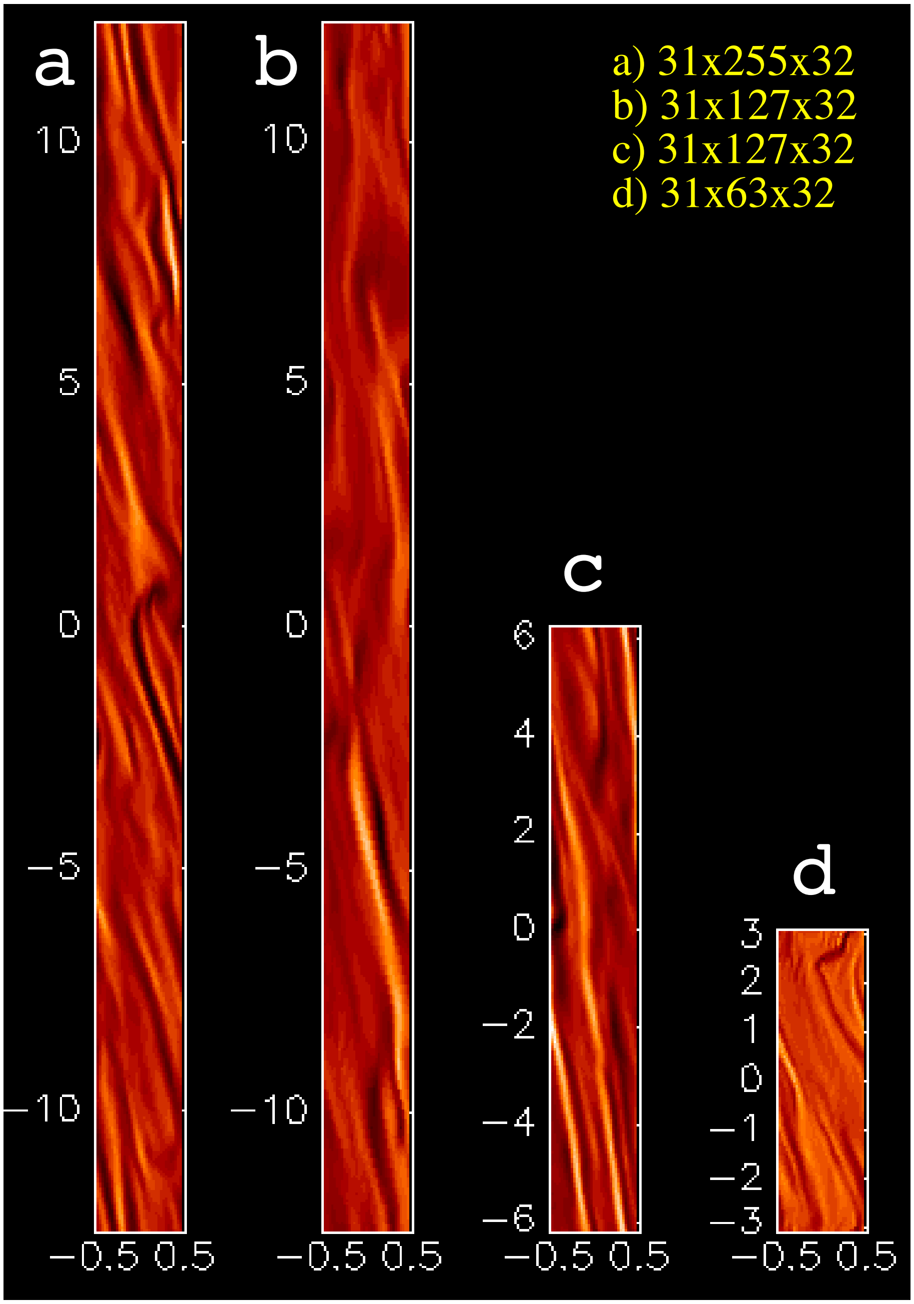

FIGURE 13. Images of vertical vorticity in horizontal planes for simulations with different toroidal extent. Note that the patterns do not seem to become longer, indicating that the most pronounced turbulence pattern is well accommodated in a box whose toroidal extent is just 2π.

5.4. *Lack of radiation transport*

The simulations of accretion disc turbulence in cartesian boxes all lack radiation transport. At best some kind of volume cooling is applied that works either in the entire computational box (BNST95) or only near the surface layers (Brandenburg *et al.* 1995b). In the former case the disc tends to be isothermal, which is clearly unrealistic. In the latter case the disc can continue to heat up in the inner parts, and only the outer parts are kept at a low temperature. This leads to a sudden drop in specific entropy near the location where the upper and lower cooling layer begin which, in turn, can lead to the development of convective layers. However, those layers do not seem to contribute significantly to the overall stress and the value of $\alpha_{\rm SS}$.

The time is ready now to incorporate realistic fully nonlocal (both optically thin and thick) radiation transport into the shearing box models. Work in this direction is currently in progress (Caunt 1998). The numerical techniques are similar to those used in solar and stellar granulation calculations (Nordlund 1982). Discs in cataclysmic variables are particularly well suited for this work, because here the temperatures and densities in the disc are comparable to those in the sun. It should in principle be possible to construct models along the upper and lower branches of the S-curve in the $(\Sigma, \nu\Sigma)$ parameter space. This would extend the one dimensional models of Meyer & Meyer-Hofmeister (1982) and Cannizzo *et al.* (1988) with prescribed $\alpha_{\rm SS}$ profiles to the three-dimensional case with self-consistently calculated turbulence without making any assumptions about the nature and properties of turbulent dissipation.

6. Questions and speculations

In this section we discuss some issues that can be addressed either now, or that one would like to address in the near future using more realistic models.

6.1. *Vortices*

Rapidly rotating bodies, such as the earth and Jupiter, show large scale vortices. In the case of the earth those vortices are associated with cyclones (low pressure) and anticyclones (high pressure), whereas in the case of Jupiter the Great Red Spot is actually an anticyclone (high pressure). It is quite possible that vortices form also in accretion discs (Abramowicz *et al.* 1992; see Bracco et al, this volume). Local simulations, however, have so far not revealed the existence of vortices (BNST95), which could be due to the inhibiting effects of the magnetic field on the development of such coherent structures (Dubrulle & Valdettaro 1992).

It has recently been proposed that vortices are a global mode of the AKA-effect (von Rekowski, Kitchatinov, & Rüdiger 1998). The AKA-effect describes an instability of the mean-field hydrodynamic equations (Frisch, She, & Sulem 1987, Kitchatinov, Rüdiger, & Khomenko 1994), similar to the α-effect in the mean-field induction equation – therefore the name AKA, which means Anisotropic Kinetic Alpha effect. Again, however, local simulations of accretion disc turbulence have not yet indicated the existence of this effect (BNST95). One possible explanation for the absence of this effect may be related to the fact that the AKA-effect requires a non-galilean invariant forcing, i.e. some forcing that moves relative to the gas in the disc. It appears difficult to explain such a forcing, unless there is a companion star constantly perturbing the velocity field.

In the nonmagnetic case Hawley (1987) found long-lived vortices in thick accretion disc simulations, and Goodman, Narayan & Goldreich (1987) found an analytic solution of a long-lived eddy, which they refer to as a planet solution. Balbus & Ricotti (1998) have extended this solution to the magnetic case with uniform pressure. However, simulations are needed to see whether or not those solutions do indeed correspond to long-lived structures.

6.2. *Relative importance of the Parker instability*

It has been debated whether or not the Parker instability plays any role in producing turbulence and to reinforcing the magnetic field. Tout & Pringle (1992) suggest that most of the *vertical* magnetic field is generated by the Parker instability. On the other hand, HGB95 have pointed out that in their simulations, since there is no vertical gravity, there is no stratification and so the Parker instability is eliminated. Therefore it can be argued that the Balbus-Hawley instability alone is sufficient to produce turbulence and reinforce the magnetic field via dynamo action without invoking the Parker instability.

Real accretion discs are stratified in the vertical direction, and thus the Parker instability will always be present. In fact, it is quite possible that it might then even contribute to driving the turbulence. To estimate the relative importance of those two mechanisms, BNST95 compared the magnitudes of the magnetic tension term, $\boldsymbol{B}\cdot\boldsymbol{\nabla}\boldsymbol{B}$, and the magnetic buoyancy term, $-\boldsymbol{\nabla}(\boldsymbol{B}^2/2)$. Unlike the case of convective dynamos (Nordlund *et al.* 1992), where the magnetic pressure gradient is larger than the magnetic tension term, BNST95 found that in discs the two are approximately equally large. They used this to suggest that Parker and Balbus-Hawley instabilities were roughly equally important for driving turbulent motions in their simulations. However, more accurate comparisons have not been carried out so far. One way to do this is to project the flow field onto the eigenfunctions of the two instabilities. A similar procedure has been adopted in the context of stellar oscillations (Bogdan, Cattaneo & Malagoli 1993).

6.3. *Protostellar discs*

Whether or not magnetic fields are of crucial importance in protostellar discs is somewhat unclear. Stepinski *et al.* (1993) argues that the degree of ionisation is so low that the conductivity will be insufficient to retain a magnetic field. If that is the case the Balbus-Hawley instability could not be responsible for driving turbulence in such discs. On the other hand, the Balbus-Hawley instability is probably the only mechanism that is known to produce turbulence and viscosity. However, self-gravity may provide another mechanism producing turbulence (Gammie, private communication).

Whether or not the Balbus-Hawley instability works depends not only on the conductivity, but also on the ratio of the neutral-ion collision frequency to the orbital frequency (Blaes & Balbus 1994). Recently, Regös (1997) has estimated that the ratio of those frequencies is around 300, large enough for the Balbus-Hawley instability to operate and for dynamo-generated turbulence to work (BNST95). Nevertheless, if the conductivity is really too low or, more precisely, the magnetic Reynolds number much below one hundred there is no way MHD effects could be important for driving turbulence, enhanced viscosity, and thus angular momentum transport.

Of course, it is possible that the estimates for the conductivity are too pessimistic. It is also possible that turbulence is really absent near the midplane of the disc, and that only the outer parts of the disc are turbulent (Gammie 1996). Furthermore, there is no doubt that both the inner parts (near the protostar) as well as the outer parts (well beyond 1 AU) are sufficiently ionised (Stepinski *et al.* 1993). Hence, in those regions MHD turbulence will be possible. This might then lead to a situation where mass is transported everywhere, except in a strip near 1 AU (for the solar nebula). This could lead to an accumulation of matter near the outer edge of the nonmagnetic strip. It is conceivable that this might then lead to an unstable situation. This type of scenario needs to be studied in more detail before some sensible conclusions can be drawn.

In any case, most parts of a protostellar disc (i.e. everywhere except near the midplane around 1 AU for the solar nebula) will be in a state of hydromagnetic turbulence. Therefore existing simulations can be used to study turbulent processes in protostellar discs such as the formation of planetesimals from dust. Hodgson & Brandenburg (1998) have recently attempted such a study. They have addressed the question whether or not dust accumulates in cyclonic vortices, as was recently suggested by Barge & Sommeria (1994) and Tanga *et al.* (1996). Similar ideas have also been put forward recently by Klahr & Henning (1997). However, the answer seems to be no for several reasons. First of all, in the simulations of BNST95 vortices are short lived, which could be due to the presence of the magnetic field (Dubrulle & Valdettaro 1992). Secondly, the strong radial shear in discs opposes the tendency for particles to accumulate in anticyclones (Hodgson & Brandenburg 1998).

An important next step in this line of research is to include agglomeration processes in such particle calculations to see whether or not turbulence enhances the collision frequency of particles to the extent that particles would stick together more easily and form planetesimals more rapidly.

6.4. *Some comments regarding 2-D models with alpha viscosity*

Traditionally the alpha-viscosity prescription has been used to construct one-dimensional accretion disc models (Shakura-Sunyaev 1973, Novikov & Thorne 1973). This approach proved to be quite successful, which is partly due to the fact that the phenomenological parameter $\alpha_{\rm SS}$ enters the final results only with low powers (e.g. Frank, King, & Raine 1992). An increase of $\alpha_{\rm SS}$ by a factor of ten would lower the disc temperature only by a factor 1.6, for example.

The alpha-viscosity has also been used to produce one-dimensional models of the vertical disc structure. In § 2.3 we have already mentioned that simulations indicate an increase of the effective value of $\alpha_{\rm SS}$ with height above the midplane. In the present section we want to discuss the use of the alpha-viscosity (or any type of turbulent viscosity) in models in more than one dimension.

It is not the dimension of the model as such that gives rise to concern, but rather the complexity of the resulting flow pattern. In one-dimensional models, and surely in some models in more than one dimension, the flow acts just in such a way as to bring the system into a relaxed state. However, in general a flow may result from some instability. For example large scale convection may be produced because of an unstable vertical or radial entropy gradient. Another obvious example of an instability is the Balbus-Hawley instability. In all those cases a curious situation may occur. Take the example of the Balbus-Hawley instability, which leads to fingering in the radial direction in a meridional plane in the presence of a vertical magnetic field (Hawley & Balbus 1991). The presence of (turbulent) viscosity may affect the onset of the instability. We refer to this instability as a macroscopic instability, so as to distinguish from the microscopic instability which was responsible for producing the turbulence, which in turn gives rise to an enhanced turbulent viscosity, ν_t.

The macroscopic instability will be suppressed when the turbulent decay rate $\nu_t k^2$ (for perturbations with wave number $\boldsymbol{k}$) becomes comparable with the growth rate of the instability, which is of the order of Ω, i.e.

$$\nu_t k^2 \gtrsim \Omega \quad \text{for macro-stability.} \tag{6.27}$$

Assuming now $\nu_t = \alpha_{\rm SS}\Omega H^2$ and $k \approx 2\pi/H$ we have

$$\alpha_{\rm SS} \gtrsim (2\pi)^{-2} \approx 0.03 \quad \text{for macro-stability.} \tag{6.28}$$

This condition is normally not satisfied, because current simulations indicate $\alpha_{\rm SS} = \mathcal{O}(0.01)$. However, we have to keep in mind that our estimates were quite crude and that $\alpha_{\rm SS}$ may turn out to be much larger in more realistic simulations. Also, of course,

$\alpha_{\rm SS}$ is time dependent, which complicates the issues further. More important at the moment seems to be the question of what is the meaning of an instability of a state that is already unstable. In the most optimistic interpretation it could mean that the turbulent state shows large scale flows, but that would mean that we have to rely on the detailed equations describing the mean flow using turbulent transport coefficients. In fact, this mean-field approach can only be, if anything, an approximation and is likely to be only of little use for any more sophisticated applications like the ones discussed here.

There is a similar example in the stellar context, where the outer convection zones are usually modelled using mixing length (or mean-field) theory. The turbulent thermal diffusivity and kinematic viscosity are given by the profiles of turbulent velocity and mixing length, that are obtained from mixing length models. One can then calculate a Rayleigh number for the convective shell and finds that it is usually supercritical. This has led to the speculation that some large scale convection might develop on top of a turbulent background and that the solar differential rotation might even be unstable (e.g. Rüdiger 1989 and references therein). In principle such large scale flows may even be physical and could resemble large scale flows that have been seen in laboratory convection (Krishnamurti & Howard 1981). Another possibility might be that, since in the sun the turbulent transport coefficients are due to convective turbulence, their values should really lead to a marginally stable state. The reason why the numbers do not quite yield a marginally stable state may be related to the fact that mean-field theories are inaccurate and do not include detailed physics such as rotation, magnetic fields, boundary effects, and the global geometry of the problem. This issue has been discussed by Tuominen *et al.* (1994), where many references to earlier work can also be found.

In conclusion, the study of flow patterns obtained by solving the mean-field hydrodynamic equations in two or even three dimensions using turbulent viscosities may be an interesting exercise, but it is at present unclear whether those flows occur in reality.

6.5. *The origin of the dynamo-alpha in discs*

We have mentioned in § 4.1 that the dynamo alpha, $\alpha_{\rm dyn}$, is negative in the upper disc plane (BNST95), which is in contrast to basic ideas in dynamo theory (e.g. Krause & Rädler 1980). The following calculation may shed some light on this question. It does reproduce the sign of $\alpha_{\rm dyn}$ that is seen in the simulations. It also yields a natural relationship between the two rather different quantities $\alpha_{\rm dyn}$ and $\alpha_{\rm SS}$.

We assume that the vertical motions are governed by magnetic buoyancy, so

$$\frac{\partial u_z'}{\partial t}=-\frac{\rho'}{\rho}g=\frac{(B^2)'}{8\pi p}g\approx\frac{\langle B_y\rangle B_y'}{4\pi p}g, \tag{6.29}$$

where primes refer to deviations from some mean value, ρ is density, p is gas pressure, and g is gravity. We adopt a local cartesian coordinate system, where y corresponds to the azimuthal direction and x to the radial direction in cylindrical polar coordinates. The resulting electromotive force is then

$$\mathcal{E}_y=\langle u_z'B_x'-u_x'B_z'\rangle\approx\langle u_z'B_x'\rangle=+\langle B_y\rangle\frac{\langle B_x'B_y'\rangle}{4\pi p}g\tau, \tag{6.30}$$

where τ is some relevant time scale. Now, because of shear ($\partial u_y/\partial x<0$) we have $\langle B_x'B_y'\rangle<0$. The dynamo alpha quantifies the magnitude of the component of the electromotive force in the direction of the mean field. Therefore,

$$\mathcal{E}_y=\alpha_{\rm dyn}\langle B_y\rangle+...,\tag{6.31}$$

and so we have (ignoring higher order terms)

$$\alpha_{\rm dyn} = +\frac{\langle B'_x B'_y \rangle}{4\pi p} g\tau. \tag{6.32}$$

In accretion disk theory the *negative* ratio of the horizontal Maxwell stress and the gas pressure is about twice the Shakura-Sunyaev viscosity parameter $\alpha_{\rm SS}$; see eq. (1.7). Also, since $g = \Omega^2 z$, we can write

$$\alpha_{\rm dyn} \approx -2\alpha_{\rm SS}\Omega^2 z\tau \tag{6.33}$$

or, in terms of the inverse Rossby number $\mathrm{Ro}^{-1} = 2\Omega\tau$,

$$\frac{\alpha_{\rm dyn}}{\Omega H} \approx -\alpha_{\rm SS}\,\mathrm{Ro}^{-1}\,\frac{z}{H}. \tag{6.34}$$

The effects of rotation and shear are now hidden in the fact that the stress $\langle B'_x B'_y \rangle$ is negative, which is due to the negative shear. This estimate also assumes that the thermal expansion of buoyant tubes is small compared with the magnetic contraction due to the $\mathbf{B}\cdot\nabla\mathbf{B}$ term. Otherwise the sign may be the conventional one. In fact, the values of $\alpha_{\rm dyn}$ obtained from the above estimate are far too optimistic compared with the values obtained in the simulations; see § 4.1. This suggests that $\alpha_{\rm dyn}$ is governed by some more delicate balance with other effects that tend to cancel each other. Thus, a proper analysis is called for. However, at present there is no other calculation that explains even the sign of $\alpha_{\rm dyn}$ that is seen in the simulations.

6.6. *Further applications, implications, and related developments*

We have mentioned in the beginning that the simulations of Balbus-Hawley turbulence and dynamo action (dynamo-generated turbulence) have had a tremendous impact on dynamo research in general. Simulations of accretion disc turbulence have produced strong large scale magnetic fields, even magnetic activity cycles, which all seem to be important properties of stellar dynamos. This has spawned related studies in at least two different directions. On the one hand, simulations of accretion disc turbulence resemble in some ways the conditions relevant to the interstellar turbulence of the stratified galactic disc on the scale of a few vertical density scale heights. On the other hand, the simulations have emphasized the importance of shear for causing large scale magnetic fields, which has led to simulations of convective stellar turbulence with imposed differential rotation with a profile similar to that suggested by helioseismology. In the following we briefly report on those two strands of ongoing investigations in a little more detail.

6.6.1. *Galaxies*

The main difference between turbulence in discs and galaxies is perhaps the presence of external drivers of turbulence in galactic discs, such as supernova explosions, stellar winds, etc. Korpi, Brandenburg, & Tuominen (1998) have recently started to investigate the effect of supernova explosions on stratified MHD shear flows with an initial toroidal magnetic field. The simulations have not yet been run for long enough, but it should be possible to assess in the near future whether the Balbus-Hawley instability leads to significant forcing of the turbulence, or whether the turbulence is mostly due to the supernova explosions or other external drivers. Longer calculations at lower resolution (Korpi *et al.* 1998) have indicated that the energy input from shear is surprisingly small compared with the energy input from supernova explosions. This is consistent with the fact that the inverse Rossby number, $\mathrm{Ro}^{-1} = 2\Omega H/\langle \boldsymbol{u}^2\rangle^{1/2}$, is much smaller in galaxies (about 1/2) than in accretion discs (20 in the simulations of BNST95).

6.6.2. *Stars*

Convective turbulence is clearly present in all late-type stars with outer convection zones. This was always thought to be the main driver of stellar dynamos. Recent simulations of Brandenburg, Nordlund, & Stein (1998) have suggested, however, that a substantial amount of energy can be tapped from the differential rotation in a similar fashion as in accretion discs. In those simulations a solar-like differential rotation profile has been added to convection simulations. Whether or not the Balbus-Hawley instability, or some other instability plays the key role is still unclear. Gilman & Fox (1997) have recently studied an instability in a sphere using a two-dimensional approach ignoring radial extent. However, this instability is unlikely to be important in the present case, because it predicts only the $m = 1$ mode to be unstable. Another proposal came from Schmitt (1985), who found that magnetostrophic waves, that are destabilized by a vertical gradient of the magnetic field, cause an α-effect which may explain the growth of large scale magnetic field seen in the simulations.

7. Conclusions

In this review we have highlighted some of the main results obtained recently using local simulations of hydromagnetic turbulence in accretion discs. The main objective for the future will be to construct global models of magnetized accretion discs. There will be two main strands of future work. On the one hand fully three-dimensional turbulence simulations will be produced that allow for realistic accretion flows and time dependence. On the other hand, local models will be improved (for example radiation transport included) and their average behaviour parameterized so that more realistic (and yet one-dimensional) accretion disc models can be constructed. Clearly, the main emphasis here will lie in combining Shakura-Sunyaev type models with dynamo models. Work in that direction has been pursued by Campbell (1992, 1997).

Already at this point some of the parameterizations suggested from simulation data have proven useful. For example the proposal that $\alpha_{\rm SS}$ is proportional to the mean magnetic energy density has been used to put constraints on models of energy extraction from rotating black holes by the Blandford-Znajek (1978) process, see Ghosh & Abramowicz (1997). Curiously enough, whilst $\alpha_{\rm SS}$ depends on the ill-known magnetic field strength, in the problem considered by Ghosh & Abramowicz the field strength drops out of the problem.

Another problem concerns the origin of turbulence in protostellar discs (i.e. is the magnetic Reynolds number large enough?) and the nature of outbursts in cataclysmic variables. Also, we would like to know the effect of the global magnetic field, which either connects with the wind of the disc or with other parts in the disc. This could significantly modify the torque acting on the disc. Global simulations should be able to address these questions.

It is a pleasure to thank my main collaborators in this field, Åke Nordlund, Bob Stein and Ulf Torkelsson for the many interesting discussions we had, especially during the Iceland meeting. I thank Eric Agol for asking me about the relative importance of compressive and vortical motions in our simulation. I am grateful to David Moss, Gordon Ogilvie, and Ulf Torkelsson for commenting on an earlier draft of this review. I am happy to acknowledge partial support from the Isaac Newton Institute, where I have written parts of this review.

REFERENCES

Abramowicz, M. A., Calvani, M. & Nobili, L. 1980 Thick accretion disks with super-eddington luminosities. *Astrophys. J.* **242**, 772-788.

Abramowicz, M. A., Brandenburg, A. & Lasota, J.-P. 1996 The dependence of the viscosity in accretion discs on the shear/vorticity ratio. *Monthly Notices Roy. Astron. Soc.* **281**, L21-L24.

Abramowicz, M. A., Lanza, A., Spiegel, E. A. & Szuszkiewicz, E. 1992 Vortices on accretion disks. *Nature* **356**, 41-43.

Agol, E. & Krolik, J. 1998 *Photon damping of waves in accretion disks.* (preprint).

Balbus, S. A. & Soker, N. 1990 Resonant excitation of internal gravity-waves in cluster cooling flows. *Astrophys. J. Letters* **357**, 353-366.

Balbus, S. A. & Hawley, J. F. 1991 A powerful local shear instability in weakly magnetized disks. I. Linear analysis. *Astrophys. J.* **376**, 214-222.

Balbus, S. A. & Hawley, J. F. 1992 A powerful local shear instability in weakly magnetized disks. IV. Nonaxisymmetric perturbations. *Astrophys. J.* **400**, 610-621.

Balbus, S. A., Hawley, J. F. & Stone, J. M. 1996 Nonlinear stability, hydrodynamical turbulence, and transport in disks. *Astrophys. J.* **467**, 76-86.

Balbus, S. A. & Ricotti, M. 1998 "On nonshearing magnetic configurations in differentially rotating disks," *Astrophys. J.* (in press).

Balbus, S. A. & Hawley, J. F. 1998 Instability, turbulence, and enhanced transport in accretion disks. *Rev. Mod. Phys.* **70**, 1-53.

Barge, P. & Sommeria, J. 1995 Did planet formation begin inside persistent gaseous vortices? *Astron. Astrophys.* **295**, L1-L4.

Bisnovatyi-Kogan, G. S. & Lovelace, R. V. E. 1997 Influence of ohmic heating on advection-dominated accretion flows. *Astrophys. J.* **486**, L43-L46.

Blandford, R. D. & Znajek, R. L. 1977 Electromagnetic extraction of energy from Kerr black holes. *Monthly Notices Roy. Astron. Soc.* **179**, 433-456.

Blaes, O. M. & Balbus, S. A. 1994 Local shear instabilities in weakly ionized, weakly magnetized disks. *Astrophys. J.* **421**, 163-177.

Bogdan, T. J., Cattaneo, F. & Malagoli, A. 1993 On the generation of sound by turbulent convection. I. A numerical experiment. *Astrophys. J.* **407**, 316-329.

Brandenburg, A. & Campbell, C. G. 1997 Modelling magnetised accretion discs. In *H. Spruit, & E. Meyer-Hofmeister* (ed. Accretion disks - New aspects), pp. 109-124. Springer-Verlag.

Brandenburg, A., Nordlund, Å., Stein, R. F. & Torkelsson, U. 1995a Dynamo generated turbulence and large scale magnetic fields in a Keplerian shear flow. *Astrophys. J.* **446**, 741-754. (BNST95)

Brandenburg, A., Nordlund, Å., Stein, R. F. & Torkelsson, U. 1995b Dynamo generated turbulence is discs. In *Small-scale structures in three-dimensional hydro and magnetohydrodynamic turbulence* (ed. M. Meneguzzi, A. Pouquet, & P. L. Sulem), pp. 385-390. Lecture Notes in Physics **462**, Springer-Verlag.

Brandenburg, A., Nordlund, Å., Stein, R. F. & Torkelsson, U. 1996a The disk accretion rate for dynamo generated turbulence. *Astrophys. J. Letters* **458**, L45-L48. (BNST96)

Brandenburg, A., Nordlund, Å., Stein, R. F. & Torkelsson, U. 1996b Dynamo generated turbulence is disks: value and variability of alpha. In *Physics of Accretion Disks* (ed. S. Kato *et al.*), pp. 285-290. Gordon and Breach Science Publishers.

Brandenburg, A., Jennings, R. L., Nordlund, Å., Rieutord, M., Stein, R. F., Tuominen, I. 1996c Magnetic structures in a dynamo simulation. *J. Fluid Mech.* **306**, 325-352.

Brandenburg, A. & Donner, K. J. 1997 The dependence of the dynamo alpha on vorticity. *Monthly Notices Roy. Astron. Soc.* **288**, L29-L33.

Brandenburg, A. & Sokoloff, D. 1998 "Local and nonlocal magnetic diffusion and alpha-effect tensors in shear flow turbulence," *Geophys. Astrophys. Fluid Dyn.* (submitted).

BRANDENBURG, A., NORDLUND, Å., STEIN, R. F. 1998 "Simulation of a convective dynamo with imposed shear," *Astron. Astrophys.* (to be submitted).

CAMPBELL, C. G. 1992 Magnetically-controlled disc accretion. *Geophys. Astrophys. Fluid Dyn.* **63**, 197-213.

CAMPBELL, C. G. 1997 *Magnetohydrodynamics in Binary Stars.* Kluwer Academic Publishers, Dordrecht.

CANNIZZO, J. K., SHAFTER, A. W. & WHEELER, J. C. 1988 On the outburst recurrence time for the accretion disk limit cycle mechanism. *Astrophys. J.* **333**, 227-235.

CAUNT, S. E. 1998, PhD thesis (University of Newcastle)

CHANDRASEKHAR, S. 1960 The stability of non-dissipative Couette flow in hydromagnetics. *Proc. Natl. Acad. Sci.* **46**, 253-257.

CHANDRASEKHAR, S. 1961 *Hydrodynamic and Hydromagnetic Stability.* Dover Publications, New York., pp. 384

COLEMAN, C. S., KLEY, W. & KUMAR, S. 1995 The oscillations and stability of magnetized accretion discs. *Monthly Notices Roy. Astron. Soc.* **274**, 171-207.

CURRY, C., PUDRITZ, R. E. & SUTHERLAND, P. 1994 On the global stability of magnetized accretion disks: axisymmetric modes. *Astrophys. J.* **434**, 206-220.

DRECKER, A., HOLLERBACH, R. & RÜDIGER, G. 1998 "Viscosity alpha in rotating spherical shear flows with an external magnetic field," *Monthly Notices Roy. Astron. Soc.* (in press).

DUBRULLE, B. 1993 On the local stability of accretion disks. *Icarus* **106**, 59-678.

DUBRULLE, B. & VALDETTARO, L. 1992 Consequences of rotation in energetics of accretion disks. *Astron. Astrophys.* **263**, 387-400.

DUBRULLE, B. & ZAHN, J.-P. 1991 Nonlinear instability of viscous plane Couette flow Part 1. Analytical approach to a necessary condition. *J. Fluid Mech.* **231**, 561-573.

FRANK, J., KING, A. R. & RAINE, D. J. 1992 *Accretion power in astrophysics.* Cambridge University Press.

FRISCH, U., SHE, Z. S. & SULEM, P. L. 1987 Large-scale flow driven by the anisotropic kinetic alpha effect. *Physica* **28D**, 382-392.

FRÖHLICH, H.-E. & SCHULTZ, M. 1996 The vertical structure of the galactic gaseous disk and its relation to the dynamo problem. *Astron. Astrophys.* **311**, 451-455.

GALSGAARD, K. & NORDLUND, Å. 1996 Heating and activity of the solar corona: I. boundary shearing of an initially homogeneous magnetic-field. *J. Geophys. Res.***101**, 13445-13460.

GAMMIE, C. F. 1996 Layered accretion in T Tauri disks. *Astrophys. J.* **457**, 355-362.

GILMAN, P. A. & FOX, P. A. 1997 Joint instability of latitudinal differential rotation and toroidal magnetic fields below the solar convection zones. *Astrophys. J.* **484**, 439-454.

GHOSH, P. & ABRAMOWICZ, M. A. 1997 Electromagnetic extraction of rotational energy from disc-fed black holes: the strength of the Blandford-Znajek process. *Monthly Notices Roy. Astron. Soc.* **292**, 887-895.

GOODMAN, J., NARAYAN, R. & GOLDREICH, P. 1987 The stability of accretion tori – II. Nonlinear evolution to discrete planets. *Monthly Notices Roy. Astron. Soc.* **225**, 695-711.

HAWLEY, J. F. 1987 Non-linear evolution of a non-axisymmetric disk instability. *Monthly Notices Roy. Astron. Soc.* **225**, 677-694.

HAWLEY, J. F. & BALBUS, S. A. 1991 A powerful local shear instability in weakly magnetized disks. II. Nonlinear evolution. *Astrophys. J.* **376**, 223-233.

HAWLEY, J. F., GAMMIE, C. F. & BALBUS, S. A. 1995 Local three-dimensional magnetohydrodynamic simulations of accretion discs. *Astrophys. J.* **440**, 742-763. (HGB95)

HAWLEY, J. F., GAMMIE, C. F. & BALBUS, S. A. 1996 Local three dimensional simulations of an accretion disk hydromagnetic dynamo. *Astrophys. J.* **464**, 690-703. (HGB96)

HODGSON, L. S. & BRANDENBURG, A. 1998 Turbulence effects in planetesimal formation. *Astron. Astrophys.* **330**, 1169-1174.

HURLBURT, N.E. & TOOMRE, J. 1988 Magnetic fields interacting with nonlinear compressible convection. *Astrophys. J.* **327**, 920-932.

KITCHATINOV, L. L., RÜDIGER, G. & KHOMENKO, G. 1994 Large-scale vortices in rotating stratified disks. *Astron. Astrophys.* **287**, 320-324.

KITCHATINOV, L. L. & RÜDIGER, G. 1997 Global magnetic shear instability in spherical geometry. *Monthly Notices Roy. Astron. Soc.* **286**, 757-764.

KORPI, M. J., BRANDENBURG, A. & TUOMINEN, I. 1998 Driving interstellar turbulence by supernova explosions. *Studia Geophys. et Geod.* (in press).

KORPI, M. J., BRANDENBURG, A., SHUKUROV, A. & TUOMINEN, I. 1998 Vortical motions driven by supernova explosions. In *P. Franco & A. Carraminana* (ed. Interstellar Turbulence), Cambridge University Press.

KLAHR, H. H. & HENNING, T. 1997 Particle-trapping eddies in protoplanetary accretion disks. *Icarus* **128**, 213-229.

KRAUSE, F. & RÄDLER, K.-H. 1980 *Mean-Field Magnetohydrodynamics and Dynamo Theory.* Akademie-Verlag, Berlin; also Pergamon Press, Oxford.

KRISHNAMURTI, R. & HOWARD, L. N. 1981 Large-scale flow generation in turbulent convection. *Proc. Natl. Acad. Sci. USA* **78**, 1981-1985.

KUMAR, S., COLEMAN, C. S. & KLEY, W. 1994 The axisymmetric instability in weakly magnetized accretion discs. *Monthly Notices Roy. Astron. Soc.* **266**, 379-385.

LIN, D. N. C. & PAPALOIZOU, J. C. B. 1980 On the structure and evolution of the primordial solar nebula. *Monthly Notices Roy. Astron. Soc.* **191**, 37-48.

LUBOW, S. H., PAPALOIZOU, J. C. B. & PRINGLE, J. E. 1994 Magnetic field line dragging in accretion discs. *Monthly Notices Roy. Astron. Soc.* **267**, 235-240.

LUFKIN, E. A., BALBUS, S. A. & HAWLEY, J. F. 1995 Nonlinear evolution of internal gravity-waves in cluster cooling flows. *Astrophys. J.* **446**, 529-540.

MATSUMOTO, R. & TAJIMA, T. 1995 Magnetic viscosity by localized shear flow instability in magnetized accretion disks. *Astrophys. J.* **445**, 767-779.

MEYER, F. & MEYER-HOFMEISTER, E. 1982 Vertical structure of accretion disks. *Astron. Astrophys.* **106**, 34-42.

NOVIKOV, I. D. & THORNE, K. S. 1973 Astrophysics of black holes. In *C. DeWitt & B. S. DeWitt* (ed. Black holes - Les astres occlus), pp. 343-450. Gordon & Breach, New York.

NORDLUND, Å. 1982 Numerical Simulations of the Solar Granulation I. Basic Equations and Methods. *Astron. Astrophys.* **107**, 1-10.

NORDLUND, Å., BRANDENBURG, A., JENNINGS, R. L., RIEUTORD, M., RUOKOLAINEN, J., STEIN, R. F. & TUOMINEN, I. 1992 Dynamo action in stratified convection with overshoot. *Astrophys. J.* **392**, 647-652.

OGILVIE, G. I. & PRINGLE, J. E. 1996 The non-axisymmetric instability of a cylindrical shear flow containing an azimuthal magnetic field. *Monthly Notices Roy. Astron. Soc.* **279**, 152-164.

PRINGLE, J. E. 1993 Cosmogony of stellar and extragalactic jets. In *Astrophysical Jets* (ed. D. Burgarella, M. Livio & C. O'Dea), pp. 1-13. Cambridge University Press.

REGÖS, E. 1997 Magnetic viscosity in weakly ionized protostellar discs. *Monthly Notices Roy. Astron. Soc.* **286**, 97-103.

RÜDIGER, G. 1989 *Differential rotation and stellar convection: Sun and solar-type stars.* Gordon & Breach, New York.

SAFRONOV, V. S. 1972 *Evolution of the protoplanetary cloud and formation of the Earth and the planets.* Israel Program for Scientific Translation, Jerusalem.

SCHMITT, D. 1985 *Dynamowirkung magnetostrophischer Wellen.* PhD thesis, University of Göttingen.

SCHRAMKOWSKI, G. P. & TORKELSSON, U. 1996 Magnetohydrodynamic instabilities and turbulence in accretion disks. *Astron. Astrophys. Rev.* **7**, 55-96.

SHAKURA, N. I. & SUNYAEV, R. A. 1973 Black holes in binary systems. Observational appearance. *Astron. Astrophys.* **24**, 337-355.

SHAPIRO, S. L., LIGHTMAN, A. P. & EARDLEY, D. M. 1976 A two-temperature accretion disk model for Cygnus X-1: Structure and spectrum. *Astrophys. J.* **204**, 187-199.

Stepinski, T. F., Reyes-Ruiz, M. & Vanhala, H. A. T. 1993 Solar nebula magnetohydrodynamic dynamos - kinematic theory, dynamical constraints, and magnetic transport of angular-momentum. *Icarus* **106**, 77-91.

Stone, J. M., Hawley, J. F., Gammie, C. F. & Balbus, S. A. 1996 Three dimensional magnetohydrodynamical simulations of vertically stratified accretion disks. *Astrophys. J.* **463**, 656-671. (SHGB96)

Tanga, P., Babiano, A., Dubrulle, B. & Provenzale, A. 1996 Forming planetesimals in vortices. *Icarus* **121**, 158-170.

Terquem, C. & Papaloizou, J. C. B. 1996 On the stability of an accretion disc containing a toroidal magnetic field. *Monthly Notices Roy. Astron. Soc.* **279**, 767-784.

Tout, C. A. & Pringle, J. E. 1992 Accretion disc viscosity: A simple model for a magnetic dynamo. *Monthly Notices Roy. Astron. Soc.* **259**, 604-612.

Tuominen, I., Brandenburg, A., Moss, D. & Rieutord, M. 1994 Does solar differential rotation arise from a large scale instability? *Astron. Astrophys.* **284**, 259-264.

van Ballegooijen, A. A. 1989 Magnetic fields in the accretion disks of cataclysmic variables. In *Accretion disks and magnetic fields in astrophysics* (ed. G. Belvedere), pp. 99-106. Kluwer Academic Publishers, Dordrecht.

von Rekowski, B., Kitchatinov, L. L. & Rüdiger, G. 1998 "Global vortex systems on standard-accretion disk surfaces," *Monthly Notices Roy. Astron. Soc.* (submitted).

Vainshtein, S. I. & Zeldovich, Ya. B. 1972 Origin of magnetic fields in astrophysics. *Sov. Phys. Usp.* **15**, 159-172.

Velikhov, E. P. 1959 Stability of an ideally conducting liquid flowing between cylinders rotating in a magnetic field. *Sov. Phys. JETP* **36**, 1398-1404. (Vol. 9, p. 995 in English translation)